European Journal of Medicinal Chemistry 124 (2016) 750–762

Contents lists available at ScienceDirect

European Journal of Medicinal Chemistry

journal homepage: http://www.elsevier.com/locate/ejmech

Research paper

Design and synthesis of chiral 2*H*-chromene-*N*-imidazolo-amino acid conjugates as aldose reductase inhibitors

Gudipudi Gopinath [a], Venu Sankeshi [b], Shaym perugu [c], Malini D. Alaparthi [d], Srinivas Bandaru [d], Vijay K. Pasala [a], Prasad Rao Chittineni [a], G.L.David Krupadanam [a, *], Someswar R. Sagurthi [d, **]

[a] Department of Chemistry, Osmania University, Hyderabad, 500 007, India
[b] Department of Zoology, Osmania University, Hyderabad, 500 007, India
[c] Department of Biochemistry, Osmania University, Hyderabad, 500 007, India
[d] Department of Genetics, Drug Design & Molecular Medicine Lab, Osmania University, Hyderabad, 500 007, India

ARTICLE INFO

Article history:
Received 4 April 2016
Received in revised form
29 August 2016
Accepted 31 August 2016
Available online 4 September 2016

Keywords:
2*H*-chromene-3-carboxylicacids
Amino acids
Imidazole
Diabetic complications
Aldose reductase inhibitor
Molecular docking

ABSTRACT

Aldose reductase (ALR2) inhibitors provide a viable mode to fight against diabetic complications. ALR2 exhibit plasticity in the active site vicinities and possible shifts in the nearby two supporting alpha helices. Therefore, a novel series of amino acid conjugates of chromene-3-imidazoles (**13**–**15**) were designed and synthesized based on natural isoflavonoids. The compounds were identified on the basis of spectral (^{1}H NMR, ^{13}C NMR and MS) data and tested *in vitro* for ALR2 inhibitory activity with an IC_{50} value ranges from 0.031 ± 0.082 μM to 4.29 ± 0.55 μM. Our *in silico* and biochemical studies confirmed that **15e** has the best inhibition activity among the synthesized compounds with a high selective index against the Aldehyde reductase (ALR1). Supplementation of **15e** to STZ induced rats decreased the blood glucose levels and delayed the progression of cataract in a dose-dependent manner. The present study thus provides novel series of compounds with a promising inhibitor to prevent or delay the cataract progression.

1. Introduction

Diabetes mellitus has surfaced as a major health issue affecting almost 300 million people across the countries [1]. A major fraction of diabetic patients suffer from long-term secondary complications such as neuropathy, nephropathy, retinopathy and cataract [2]. Diverse pathways and regulatory networks have been proposed in diabetic patients, of particular relevance, the polyol pathway which happens to first discovered, is still a generally accepted as the mechanism of prime importance in the diabetic complication and pathogenesis [1,3]. Seminal studies by Kinoshita et al., way back in 1965 demonstrated the involvement of ALR2 (polyol pathway) in the development of cataractous lens [4] and till date forms the most common mechanism in cataract pathogenesis. Multiple mechanisms that manifest in the pathogenesis of diabetic cataract which includes inhibition of aldose reductase (ALR2; EC: 1.1.1.21) has now become a potential pharmacological target [5–7]. In normal physiological conditions, the cellular glucose is metabolized through glycolysis pathway, however, an investigation by Van Heyningen 1959, showed the dynamic involvement of pentose shunt pathway, which is now observed as a crucial pathway regulating in human cataract as well [8]. During hyperglycemic conditions, the increased amount of glucose activates an ALR2 which forms the first rate-limiting enzyme of polyol pathway. ALR2 utilizes a large amount of intracellular NADPH to catalyze the reduction of glucose to sorbitol, which is the initial or the primary step in polyol pathway [9]. The downstream effects involving increased flux of glucose through the polyol pathway trigger the accumulation of sorbitol. The hyperosmotic effects of sorbitol accumulation owing to its polar nature, eventually leads to lens swelling, damage and change in membrane permeability. In addition, the drastic reduction of NADPH forms an important cofactor for reviving critical intracellular antioxidants and reduced glutathione levels. An emerging

* Corresponding author. Department of Chemistry, Natural Product lab, Osmania University, Hyderabad, 500 007, India.
** Corresponding author. Department of Genetics, Drug Design & Molecular Medicine Lab, Osmania University, Hyderabad, 500 007, India.
E-mail addresses: gldkrupa@gmail.com (G.L.David Krupadanam), drsomeswar@osmania.ac.in (S.R. Sagurthi).

http://dx.doi.org/10.1016/j.ejmech.2016.08.070
0223-5234/

evidence suggests that by dropping the amount of reduced glutathione in hyperglycemic conditions, the polyol pathway increases susceptibility to intracellular oxidative stress, which results in diabetic cataract by activation of enzyme aldose reductase [10–13].

Noticeably, most of the ALR2 inhibitors (ARIs) are pharmacologically control the abnormal accumulation of sorbitol and may indirectly inhibit oxidative stress. A large variety of structurally diverse compounds have been identified as potent inhibitors to ALR2. The well characterized ALR2 inhibitors from the earlier studies has been classified into three main chemical classes: (i) carboxylic acid derivatives, such as Epalrestat [14], Tolrestat [15], Zopolrestat [16] and Zenarestat [17]; (ii) spiro-hydantoins, such as Sorbinil [18,19], Fidarestat [20]; Ranirestat [21] (iii) natural phenolic derivatives, such as Quercetin [22] and their methyl ethers as well as glycosides [22] (Fig. 1). Nevertheless, many of them are lacking specificity and sensitivity towards the human ALR2 and also penetration issues with the target tissues [23]. To the date, there are no any FDA-approved drugs against human ALR2. However, in the recent years, Ranirestat progressed to the late phase of clinical trials [24]. Unfortunately, none of the proven ARI's have not shown sufficient efficacy in human clinical trials and also failed with undesirable side effects. In the pursuit for better ARIs, there has been a paradigm shift towards novel chemical moieties, which can accommodate the anionic and specific binding pockets (Fig. 2) of ALR2 [25]. In the first part of this study, the flexible and adaptable active site properties of ALR2 were analyzed with the help of multiple crystal structures. The binding pocket of aldose reductase consists of a rigid anion binding pocket and a flexible specificity pocket. The anion-binding pocket is formed mostly by His 110, Tyr 48, Trp 111 and the positively charged NADP+. The binding pocket may only be opened by inhibitors that offer the right interactions. The amino acids, Phe 122 and Leu 300 which otherwise serve as gatekeepers and can seal the pocket, however, the main flexibility is conferred by the Ala 299-Leu 300 backbones and is apparent in different conformations of the Leu 300 side chain which determines the open or closed conformation of the pocket. It was demonstrated that ALR2 with citrate (PDB code: 1X96) [26] exhibited specificity pocket in the closed conformation and however open conformation in another crystal structure (PDB code: 1US0) [27]. The plasticity of an ALR2 enzyme was well characterized, with soaked co-crystal structures by using Zopolrestat and Tolrestat as inhibitors. The peptide flip is accompanied by a rupture of an H-bond formed to the bound ligand Zopolrestat (PDB code 2DUX) [28]. In the recent studies, it was shown that two molecules of inhibitors (indole-1-acetic acid derivatives) were accommodated in the binding site of ALR2 (PDB code: 4QX4) [29]. The AR crystals soaked with Tolrestat, enzyme found to hold four molecules of Tolrestat in the active site and binding site's proximity (PDB code: 2FZB) [28], which is possible by pronounced shifts concerning two helices interacting with the additional ligands and crystal packing, most likely originating from protein flexibility resulting in different geometries in deviating environments. Protein adaptability is an important prerequisite for biological function. Nevertheless, it also provides a special challenge to inhibitor design as flexibility complicates the prediction of the binding mode of a small molecule ligand. In line with the above findings, we used a strategy to search for novel ARIs with the hypothesis that the combination of two proven moieties in one single compound may result in a molecule of choice to treat diabetes and related diabetic secondary complications. In this study, taking consideration of the ALR2 enzyme flexibility and dynamic properties we designed a new series of compounds from proven AR inhibitors. Present novel series consists of fragments from Sorbinil, Fidarestat and Quercetin (Fig. 3). The synthesized compounds were subjected to docking studies towards Human ALR2 enzyme to evaluate their affinity and binding interaction in the active site. The compounds were evaluated *in-vitro* and most potent inhibitor from this novel series was assessed *in-vivo* for its ability to delay or prevent the progression of cataract.

2. Results and discussion

2.1. Synthesis

The salicylaldehyde and 3-Methoxysalicylaldehyde (*o*-vanillin) (**1a,b**) reaction with acrylonitrile in the presence of 1,4-diazabicyclo [2.2.2]octane (DABCO) gave substituted-2*H*-chromene-3-nitriles (**2a,b**), these substituted-2*H*-chromene-3-nitriles (**2a,b**) were hydrolyzed to substituted-2*H*-chromene-3-carboxylic acids (**3a,b**) [30], (Scheme 1). The *tert*-butyl(5-aryl-1*H*-imidazol-2-yl)alkyl carbamates (6**a-e, 7a-b** & **8a–c)** were synthesized by the reaction of substituted phenacyl bromides (**5a-f**) [30] with *N*-Boc-amino acids (**4a–c**) (like *N*-Boc-glycine (**4a**), *N*-Boc-valine (**4b**) and *N*-Boc-proline (**4c**) in the presence of TEA, followed by refluxed with ammonium acetate in toluene [31] (Scheme 2). Substituted-2*H*-chromene-3-carboxylic acids (**3a-b**) were reaction with $SOCl_2$ to get the corresponding acid chlorides (**9a, b**) and *tert*-butyl(5-aryl-1*H*-imidazol-2-yl)alkyl carbamates (**6a-e, 7a-b** & **8a–c**) on treatment with TFA gave the corresponding Boc deprotected amines (5-aryl-1H-imidazol-2-yl)alkylamine) as their TFA salts (**10a–e, 11a–b** & **12a–c**). The targeted compounds *N*-((5-substituted phenyl-1*H*-

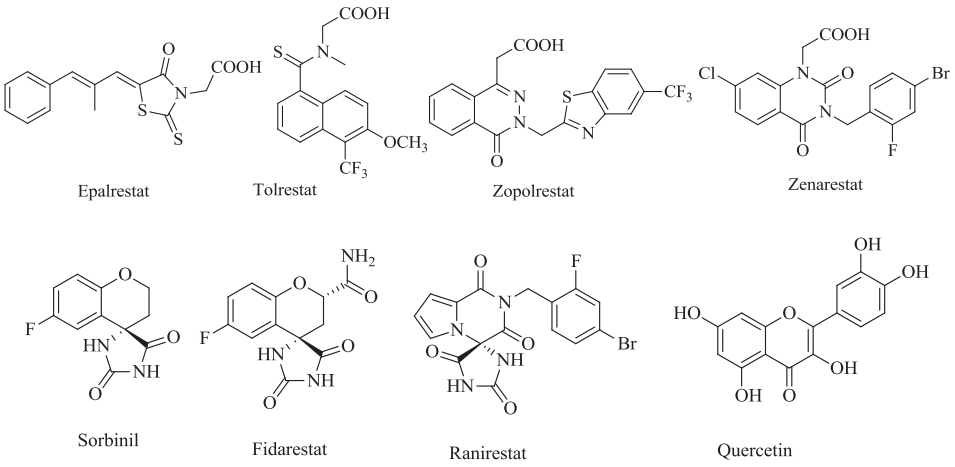

Fig. 1. Proven Aldose reductase inhibitors.

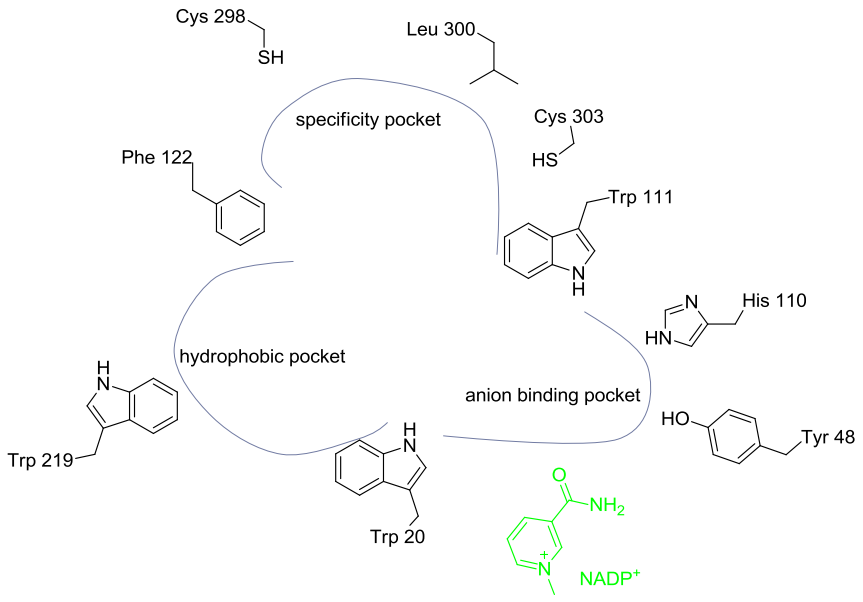

Fig. 2. Schematic view of the binding site of ALR2. The anion binding pocket is mainly formed by Tyr 48, His 110, Trp 111, and NADP+. The specificity pocket is opened and closed because of the conformational changes in the backbone of the Phe 122, Cys 296, Leu 300 and Cys 303. The hydrophobic pocket is formed by Trp 219 and Trp 20.

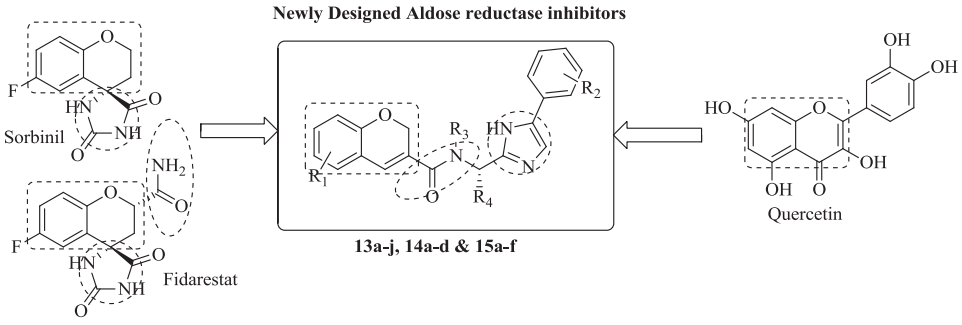

Fig. 3. Designed ALR2 inhibitors as hybrids of Sorbinil, Fidarestat and quercetin.

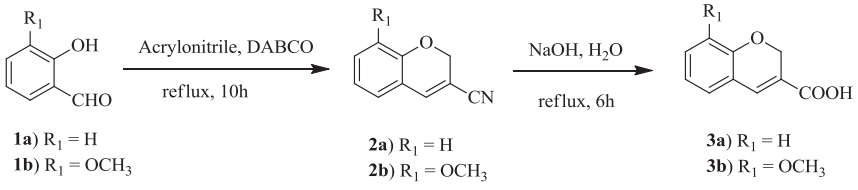

Scheme 1. Synthesis of substituted-2*H*-chromene-3-carboxylic acids (**3a-b**).

imidazol-2-yl)alkyl)-2*H*-chromene-3-carboxamides (**13a–j, 14a–d & 15a–f**) were obtained from the reaction of chromene-3-carboxylic acid chlorides (**9a, b**) with appropriate aryl imidazole amines (**10a–e, 11a–b & 12a–c**) in the presence of TEA (Scheme 3).

2.2. Biological studies

All newly synthesized derivatives of *N*-(imidazole)-2*H*-chromene-3-carboxamides derivatives (**13a–j, 14a–d & 15a–f**) were screened for their effective inhibitory potential against ALR1 and ALR2 enzymes, extracted from rat kidney and lenses, respectively, and purified. All the compounds were subjected against both enzymes in order to determine their selectivity. In addition, to know the inhibitory effect of compound **15e** was evaluated for *in-vivo* AR activity.

2.2.1. In vitro ALR1 and ALR2 activity

The *N*-(imidazole)-2*H*-chromene-3-carboxamides derivatives (**13a–j, 14a–d & 15a–f**) were tested in *in-vitro* against the inhibition of aldose reductase (ALR2) and aldehyde reductase (ALR1) with Sorbinil [32] and Valproic acid [33] as positive controls. The enzymes ALR1 and ALR2 share 65% similarity of amino acid residues with some differences in their respective active sites, which makes it difficult in designing inhibitors with selectivity and ultimately leading to toxicity issues [34]. Most of the synthesized compounds (**13a–j, 14a–d & 15a–f**) were having selectivity as evidenced by IC_{50} values ranging from 0.031 ± 0.082 μM to 4.29 ± 0.55 μM (Table 1). Among all the derivatives, **15e** is found to be the most potent with an 8-methoxy group on chromene nucleus, 4-chlorophenyl on imidazole and with pyrrolidine spacer between chromene, imidazole moieties against ALR2 inhibition.

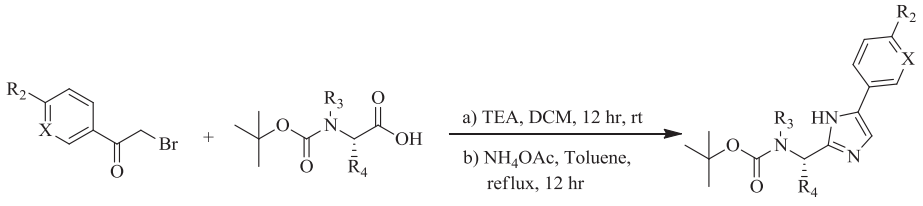

4a) R_2= H, X=C
4b) R_2= Cl, X=C
4c) R_2= Br, X=C
4d) R_2= F, X=C
4e) R_2= OCH_3, X=C
4f) R_2= H, X=N

5a) BOC-Gly-OH (R_3=R_4=H)
5b) (S)-BOC-Val-OH (R_3=H, R_4=-$HC(CH_3)_2$)
5c) (S)-BOC-Pro-OH (R_3=R_4=-CH_2-CH_2-CH_2-)

6a) X=C, R_2=R_3=R_4= H,
6b) X=C, R_2= Cl, R_3=R_4= H
6c) X=C, R_2= Br, R_3=R_4= H
6d) X=C, R_2= F, R_3=R_4= H
6e) X=C, R_2= OCH_3, R_3=R_4= H
7a) X=C, R_2=R_3=H, R_4= -$HC(CH_3)_2$
7b) X=C, R_2= Br, R_3=H, R_4= $HC(CH_3)_2$
8a) X=C, R_2=R_3=R_4= -CH_2-CH_2-CH_2-
8b) X=C, R_2= Cl, R_3=R_4= -CH_2-CH_2-H_2-
8c) X=N, R_2=H, R_3=R_4=-CH_2-CH_2-CH_2-

Scheme 2. Synthesis of *tert*-butyl (5-aryl-1*H*-imidazol-2-yl)alkylcarbamate (**6a-e, 7a, b & 8a–c**).

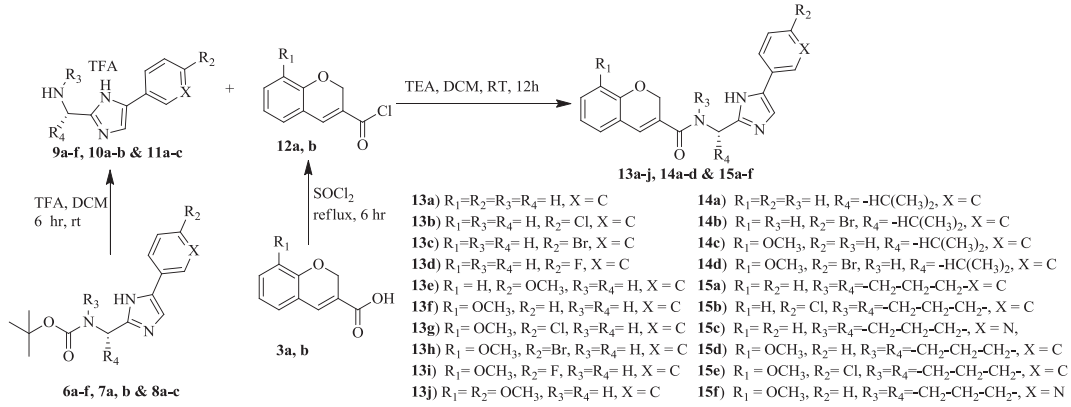

13a) R_1=R_2=R_3=R_4= H, X = C
13b) R_1=R_3=R_4= H, R_2= Cl, X = C
13c) R_1=R_3=R_4= H, R_2= Br, X = C
13d) R_1=R_3=R_4= H, R_2= F, X = C
13e) R_1 = H, R_2= OCH_3, R_3=R_4= H, X = C
13f) R_1= OCH_3, R_2= H, R_3=R_4= H, X = C
13g) R_1= OCH_3, R_2= Cl, R_3=R_4= H, X = C
13h) R_1 = OCH_3, R_2=Br, R_3=R_4= H, X = C
13i) R_1= OCH_3, R_2= F, R_3=R_4= H, X = C
13j) R_1= R_2= OCH_3, R_3=R_4= H, X = C

14a) R_1=R_2=R_3= H, R_4= -$HC(CH_3)_2$, X = C
14b) R_1= R_3=H, R_2= Br, R_4= -$HC(CH_3)_2$, X = C
14c) R_1= OCH_3, R_2= R_3=H, R_4= -$HC(CH_3)_2$, X = C
14d) R_1= OCH_3, R_2= Br, R_3=H, R_4= -$HC(CH_3)_2$, X = C
15a) R_1= R_2= H, R_3=R_4=-CH_2-CH_2-CH_2-X = C
15b) R_1=H, R_2= Cl, R_3=R_4=-CH_2-CH_2-CH_2-, X = C
15c) R_1= R_2= H, R_3=R_4=-CH_2-CH_2-CH_2-, X = N,
15d) R_1= OCH_3, R_2= H, R_3=R_4=-CH_2-CH_2-CH_2-, X = C
15e) R_1 = OCH_3, R_2= Cl, R_3=R_4=-CH_2-CH_2-CH_2-, X = C
15f) R_1 = OCH_3, R_2= H, R_3=R_4=-CH_2-CH_2-CH_2-, X = N

Scheme 3. Synthesis of *N*-((5-substituted phenyl-1*H*-imidazol-2-yl)alkyl-2*H*-chromene-3-carboxamides (**13a–j, 14a–d & 15a–f**).

Table 1
Inhibitory Effect of Compounds **13**–**15** on Rat ALR2 and ALR1and selectivity index.

Compound	IC_{50} values (μM) of ALR2[a]	IC_{50} values (μM) of ALR1[a]	Selectivity Index[b] (ALR1 IC_{50} ±SD/ALR2 IC_{50} ± SD)
13a	2.122 ± 0.14	5.193 ± 0.22	2.477
13b	0.114 ± 0.031	2.421 ± 0.022	21.23
13c	0.732 ± 0.023	3.381 ± 0.01	4.61
13d	0.42 ± 0.011	1.842 ± 0.062	4.385
13e	0.275 ± 0.01	2.537 ± 0.070	9.22
13f	0.731 ± 0.027	1.215 ± 0.059	1.66
13g	0.065 ± 0.033	1.441 ± 0.062	22.16
13h	0.091 ± 0.076	1.558 ± 0.007	17.12
13i	0.071 ± 0.082	1.621 ± 0.081	22.83
13j	0.899 ± 0.02	1.311 ± 0.022	1.45
15a	3.67 ± 0.54	5.719 ± 0.26	1.55
15b	0.337 ± 0.042	3.882 ± 1.32	11.51
15c	0.222 ± 0.049	2.432 ± 0.097	10.95
15d	3.072 ± 0.65	1.831 ± 0.074	0.596
15e	**0.031 ± 0.082**	**3.422 ± 0.081**	**110.39**
15f	0.146 ± 0.077	1.418 ± 1.03	9.712
14a	4.29 ± 0.55	9.412 ± 0.037	2.193
14b	0.22 ± 0.082	2.277 ± 0.046	10.35
14c	1.0 ± 0.6	4.873 ± 0.01	4.87
14d	0.771 ± 0.011	3.408 ± 0.005	4.42
Sorbinil[c]	0.43 ± 0.014	–	
Valproic acid[d]	–	53.1 ± 0.55	

[a] $n = 5$.
[b] Defined as IC_{50}[ALR1]&IC_{50}[ALR2].
[c] Reported IC_{50} of 0.43 μM by Ref. [32].
[d] Reported IC_{50} of 53.1 ± 0.55 mM [33].

Among the series **13a**–**j** (glycine conjugates), compound **13g** was the most potent inhibitor of ALR2, possessing an IC_{50} value of 0.065 ± 0.033 μM. Compound **13g** has a chlorine atom attached to the phenyl group over imidazole and methoxy on chromene both separated by carboxamide. A slight decrease in activity was observed when the chlorine atom was replaced with a bromine, fluorine group in compound **13h** & **13i** (IC_{50} values: 0.091 ± 0.076 & 0.079 ± 0.082 μM), and without methoxy group on chromene nucleus decrease in the activity compared methoxy containing analogs, resulting in fewer interactions with the active site of aldose reductase, the compounds without any substitution (**13a**) on the phenyl ring of the imidazole fragment and chromene has exhibited lesser activity. Whereas among the series **14a**–**d** derived from L-valine, these compounds have exhibited lesser activity compared to other compounds.

In the series **15a**–**f**, compound **15e** with IC_{50} values of 0.337 ± 0.042 μM respectively, were found more potent inhibitors of ALR2 than the standard inhibitor, Sorbinil. The higher activity may be assigned to the presence of imidazole ring with *para*-chloro substituted phenyl ring pendant is separated by a pyrrolidin-2-yl amide linkage from the chromene at 3rd position resulting in a more potent structure that gives stronger interactions with the active site for binding.

2.2.2. Selectivity

The test for selectivity over the closely related aldehyde reductase (EC.1.1.1.2, ALR1) was carried out. The ALR1 inhibitory potencies (expressed as IC_{50}) were calculated in the reduction of the substrate D-glucuronate by partially purified ALR1 from rat kidney, are shown in Table 1. For comparison, the reference Valproic acid was included. All tested compounds (**13a**–**j**, **14a**–**d** & **15a**–**f**) were shown less inhibitory activity with ALR1 compared to ALR2. In the series of the most efficient ARIs, the selectivity indices were found to be the highest for the compound **15e**. In all these analogs tested against ALR2 chromene moiety is represented with a 3 atom amide linkage, of which amide carbonyl originates from chromen-3-acid chloride and the other part from L-amino acids (glycine, valine & proline). Therefore, among the glycine derivatives (**13a**–**j), 13b & 13g** compounds with 4-chlorophenyl substituted on imidazole exhibited highest IC_{50} values 0.11 ± 0.03 & 0.07 ± 0.03 respectively. In valine derivatives (**14a**–**d**), 4-bromophenyl substituted imidazole derivatives **14b & 14d** have shown IC_{50} values 0.22 ± 0.08 & 0.77 ± 0.01 respectively. In the entire group of compounds **15e** with 8-OMe & 4-chlorophenyl substituted has exhibited the highest activity, suggesting that the most hydrophobic nature of the substrates has helped in enhancing the activity. In proline derivatives, **15b** with 4-chlorophenyl substituted on imidazole ring has shown better activity with IC_{50} = 0.34 ± 0.04. The interesting compounds were observed in **15c** with a 3-pyridinyl ring on imidazole which has shown further improvement in the activity (IC_{50} = 0.22 ± 0.05). But this trend is lost with the presence of 8-OMe group on chromene moiety (**15e**: IC_{50} 0.03 ± 0.08, **15f**: IC_{50} = 0.15 ± 0.08). Nevertheless, important functional considered from *in-vitro* studies on this scaffold is the 4-chlorophenyl, which has enhanced the activity irrespective of the substitutions in the carboxamide linker. Hence, **15e** is more potent under *in vitro* studies over Sorbinil which requires further exploration of treatment of diabetic secondary complications. But against the ALR1, even though the similar trends were observed the IC_{50} values are higher, indicating the selective of their compounds, towards ALR2 over ALR1. It should be noted that the most selective compound **15e**, with a selectivity factor above (110.4), is also the most potent ARI in this series. It is an important feature of selectivity over the other members of the aldo-keto reductase family. The non-inhibition of structurally related physiologically relevant oxidoreductases may minimize the undesired side effects.

2.3. Molecular docking studies

Human ALR2 crystal complexes have suggested that the inhibitors bind to the enzyme active site and are held in place through hydrogen bonding and van der Waals interactions formed within the hydrophobic pockets [35]. These ligand-dependent conformations indicate a remarkable induced fit or flexibility of the active site in the human ALR2 from the earlier studies (PDB codes: 1Z3N & 1US0). Three binding pockets were proposed at the active site of ALR2 based on the X-ray crystallography and mutagenesis [36]. The first site is usually occupied by the anion head of ligand and thus named “anion binding pocket”. It consists of Tyr48, His110, Trp20, and Trp111 side chains and the positively charged nicotinamide moiety of the cofactor $NADP^+$ [37]. The second is a hydrophobic pocket, known as specificity pocket, and lined by the residues Leu 300, Cys 298, Cys 303, Trp 111, Cys 303, and Phe 122. The specificity pocket displays a high degree of flexibility and the third is another hydrophobic pocket formed by the residues Trp 20, Trp 111, Phe 122, and Trp 219 [38a]. By using above information we defined the ligand binding cavities and carried out docking studies by Schrodinger. Similar information was obtained from the ALR1 crystal structure (PDB code 3H4G) [38b] and defines the binding sites carried out the comparative studies (Table 2). Molecular docking studies were carried out to substantiate the interacting patterns and selectivity of synthesized compounds with the ALR2 and ALR1.

2.3.1. Structural activity relationship

All the compounds were docked against ALR2 in which the glycine spacer series (**13a**–**j)** have lower affinity than valine spacer series **14a**–**d,** whereas these two series exhibited lower affinity towards the enzyme when compared to the proline spacer series (**15a**–**f).** In the **13a**–**j**, **13f**–**j** has a higher affinity towards ALR2, owing to the presence of 8-methoxy group on the chromene ring and substituted phenyl group on the imidazole. Among **13g**–**i** side chain exhibited higher affinity in which *para*-fluoro phenyl group (**13i)** and methoxy phenyl group on imidazole (**13j)** compounds have shown maximum affinity with a docking score of −8.79 and −8.68, respectively. In the **14a**–**d,** 4-bromophenyl substituted derivatives (**14b & 14d)** on imidazole has shown a slightly lower affinity, but the presence of 8-methoxy group on the chromene ring **14c** has improved the affinity with a docking score of −8.87. The **15a**–**f** showed a maximum affinity towards ALR2 with a docking score ranging from −8.12 to −9.35. In the **15** series the 4-chlorophenyl substituted imidazole derivatives **15b** and **15e** exhibited higher affinity with docking scores of −8.97 and −9.35. But, the 3-pyridinyl ring on the imidazole of **15c** and **15f** showed decreased affinity towards ALR2 with a score of −8.12 and −8.81 in comparison with their respective 4-chlorophenyl substituted imidazole derivatives **(15b** & **e)**. The addition of 8-methoxy group

Table 2
Molecular docking scores of compounds screened against ALR1 (PDB code: 3H4G) and ALR2 (PDB code: 1Z3N).

S. No	Mol dock score		S. No	Mol dock score	
	ALR1	ALR2		ALR1	ALR2
13a	−4.13	−7.79	**14a**	−4.35	−8.57
13b	−4.3	−7.59	**14b**	−4.13	−8.34
13c	−4.12	−6.97	**14c**	−4.54	−8.87
13d	−5.6	−7.12	**14d**	−5.9	−8.63
13e	−4.8	−7.86	**15a**	−6.0	−8.75
13f	−7.0	−8.06	**15b**	−6.6	−8.97
13g	−5.9	−8.71	**15c**	−5.9	−8.12
13h	−5.7	−8.28	**15d**	−6.3	−8.89
13i	−6.03	−8.79	**15e**	**−6.38**	**−9.35**
13j	−6.0	−8.68	**15f**	−7.0	−8.81

on the chromene ring and 4-chlorophenyl on imidazole derivative (**15e**) has shown an utmost affinity with the highest docking score of −9.35. Further, a closer look at the active molecule indicates that the presence of 8-methoxy group on the chromene ring and a halogenated phenyl group on the imidazoles have a higher affinity towards ALR2. C. Nantasenamat et al. demonstrated that halogens are essential for the observed ALR2 inhibitory activity, which is further supported by K. Ko & Y. Won and B. Vyas et al. In their studies also halogenated compounds and specifically chlorine derivatives had shown the highest inhibitory activity [39a–c]. In our results (Table 1) the constant and coefficient values used in are in higher end, even in the earlier studies had shown that there have been QSAR models for ARI's reported with larger constant values than that in our results. In the example, Soni and Kaskhedikar reported a QSAR model for 2,4dioxo5(naphtha2ylmethylene)3thiazolidinylacetic acids and 2thioxoanalogues as $pIC_{50} = 6.634 + 0.504\ \Sigma\pi + 0.659\ I_x$ ($r^2 = 0.726$) [39d]. More recently, Nantasenamat et al. reported a QSAR model with a much larger constant value, 6.766, and much smaller coefficients of explanatory valuables (0.0970.332) to predict aldose reductase inhibitory activity of sulfonylpyridazinones [39b]. The **15e** molecule which is foreseen to be the best ARI also has a 4-chlorophenyl substitution. Drug likeliness and Physico-chemical properties of the molecules were also calculated and incorporated in the supplementary data.

2.3.2. Docking analysis of 15e and structural superposition

It was observed that **15e** docked well in the active site of ALR2 with a better docking score (−9.3) compared to any other compound. It interacts with ALR2 at active site residues Trp 20, Val 47, His 110, Trp 111 and Lue 300 (hydrogen bond distance 2.5, 2.3, 3.0, 2.8, 2.9 Å, respectively) (Supplementary data). **15e** compound has several electrostatic (Trp 20, Val 47, Trp 111, Thr113, Pro 218) and van der Waal interactions (Lys 21, Tyr 48, Gln 49, Trp 79, Cys 80, His 110, Phe 122, Trp 219, Cys 298, Cys 303, Thr 309 and Phe 311) (Fig. 4a). Hence, it appears that **15e** compound might bind to ALR2 in a both conformation (the open conformation figure is incorporated in supplementary data) these can be confirmed by co-crystallization of **15e** with ALR2. In the case of ALR1, hydrogen bonding was observed between and amino acid residues Trp 22, Trp 114 Met 302 and Arg (bond distance less than 3.20 Å) (Fig. 4b). Since Trp-20/Arg 312, Trp 111/Trp 22, His 110/Asn 163 were replaced in ALR1, **15e** did not interact with His 110 and Trp 20. It is interesting to note that unlike with ALR1, **15e** interacted with Leu 300 and Leu 301 in ALR2 those are involved in imparting plasticity to ALR2. We have performed docking with the open and closed conformation of ALR2 crystal structures as augmented in supplementary data. The compound **15e** was docked in reference to a co-crystallized compound in the PDB structures which shows least Root mean square deviation (as determined by OPLS force-fields) demonstrating it to fit best in the active site.

In addition, **15e** shows the superior docking score in both open (PDB-1US0, docking score −10.34) and closed conformations of the protein which confirms its high binding affinity. In addition, the high affinity of compounds can be further testified by its optimal potential energy, columbic and van der Waals forces, interaction profile as well as excellent hydrogen bonding efficiency in the active site of the protein. The molecular alignment was performed with the highest dock scored compound **15e** was used as the template and all the other proven (Fidarestat, Sorbinil and Zopolrestat) on the common core (Fig. 5a). Occupancy and spacial arrangement of **the 15e** compound were compared Tolrestat soaked crystal (PDB code: 2FZB (Fig. 5b)). **15e** molecule nearly covered the vicinity of two molecules of Tolrestat (Fig. 5b). From the binding analysis of the 15e molecule with open and closed conformations anticipated answering the induced-fit properties of the

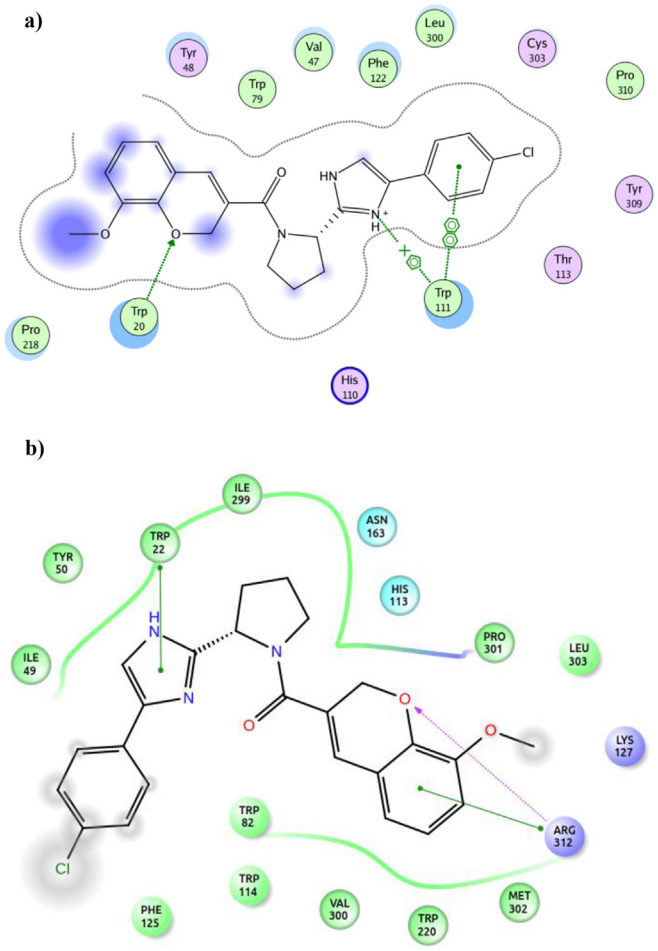

Fig. 4. a: 2D representation of **15e** interactions with the ALR2 active site pocket in closed conformation (PDB code 1Z3N). **b**: 2D representation of **15e** interactions at the active site of ALR1 (PDB code 3H4G).

ALR2 [39a,b]. These *in-silico* assumptions have to be proved by co-crystallization studies.

2.4. Delayed cataract progression in STZ induced rats

In order to know the inhibitory effect of compound **15e** in *in-vivo*, the following experiment was performed by following earlier standardized protocols [40]. Rats were divided into six groups (each group $n = 12$), Group-I: normal control rats, Group-II: diabetic control rats, Group-III & Group-IV: diabetic rats were fed with 5 and 50 μM/kg body weight of the **15e** compound, respectively. Group-V (Sorbinil 50 μM/kg) & Group-VI (Fidarestat 50 μM/kg body weight) diabetic rats were fed with known AR inhibitors. All rats (Group I-IV) were fed with ad libitum and it was noticed that there was an increase in food intake in all diabetic rats (Group II-VI). Despite increased food intake, the body weight of diabetic rats was found low (Group-II 186 ± 6.91 g), in relation to the control (Group-I 350 ± 6.33 g) and compound **15e** fed rats (Group-III 309 ± 10.1 g and Group-IV 320 ± 3.17 g, Fig. 6). Elevated blood glucose levels have been attenuated by feeding with compound **15e** (Group-III 138.86 ± 6.20 mg/dl, Group-IV 129.80 ± 3.56 mg/dl Vs Group-II 261.53 ± 53 mg/dl, Fig. 7). At the end of 8 weeks, we have noticed a decrease in AR activity in Group-III and IV rats in a dose-dependent manner (Table 3). On an extended feeding of compound **15e** to diabetic rats, we have noticed a delay in the progression of

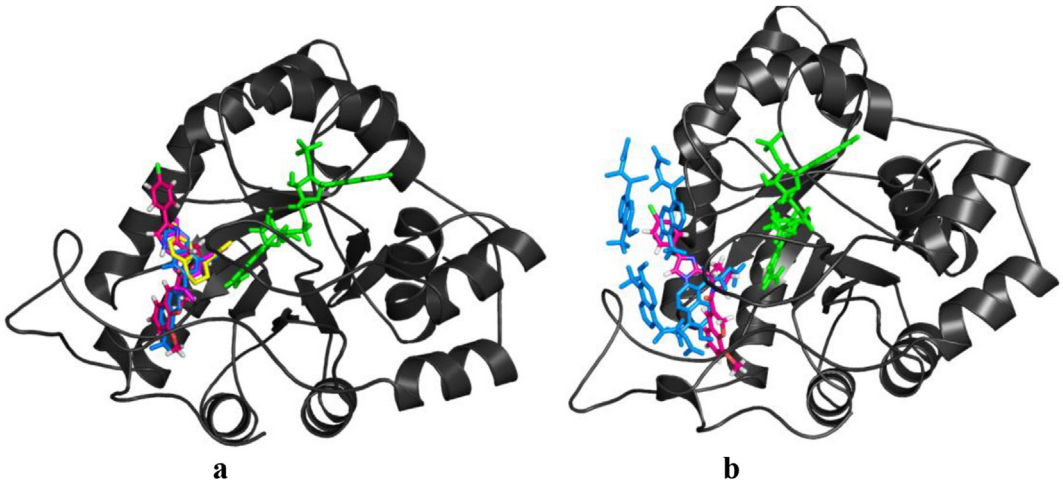

Fig. 5. a & b: Structural alignment of known ARIs in comparison to **15e**. (a) Inhibitors represented in stick model in the active site, **15e** is shown in pink, Sorbinil (PDB code 1AHO), Fidarestat (PDB code 1PWM) and Zopolrestat (PDB code 2DUX) are shown in yellow, magenta and marine blue, respectively. (b) The soaked crystals of ALR2 with tolrestat (marine blue color) accommodated four inhibitor molecules (PDB code 2FZB) at the binding pockets. This PDB superposed with **15e** (magenta color) docked ALR2 structure. (For interpretation of the references to colour in this figure legend, the reader is referred to the web version of this article.)

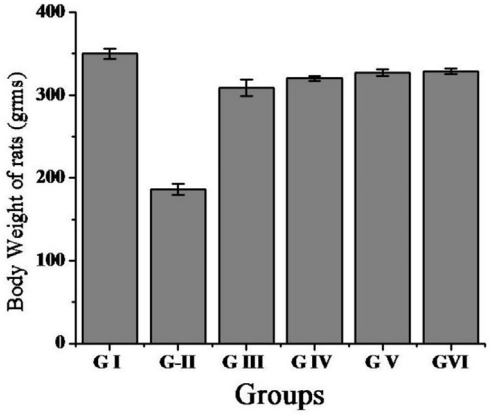

Fig. 6. Effect of **15e** on the body weight of different groups (I-VI) in diabetic rat lens. Experimental diabetes was induced with a single dose of Streptozotocin (IP 32 mg/kg body. Wt) and diabetic rats were maintained for 8 weeks with or without dietary supplementation of compound **15e**. Body weights were measured weekly basis in different groups (G- I to G-VI) of rats. The compound **15e** supplemented (G- III & G -IV) and Sorbini (G-V) & Fidarestat (G-VI) rats body weights were compared with control (G–I) and diabetic rats (G- II).

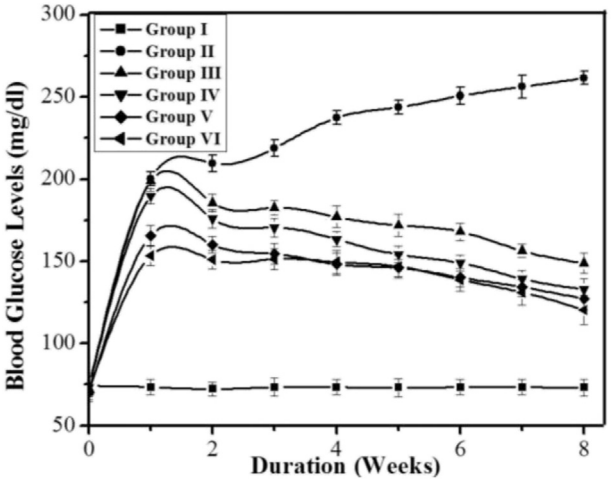

Fig. 7. Estimation of blood glucose levels in control (Group I; uninduced) and STZ induced diabetic rats (Group II to Group VI). Experimental diabetes was induced with a single dose of Streptozotocin (STZ) (IP 32 mg/kg body weight) and all rats were maintained for 8 weeks. In Group I – control uninduced rats, Group –II to VI all were STZ induced rats, Group III & IV supplemented with 15e with the concentration of 5 μM & 50 μM, respectively. In the groups V & VI, supplemented with Sorbinil and Fidarstat with 50 μM each. Blood glucose levels were measured each group on a weekly basis to assess the diabetic conditions in different groups of rats (Group I to Group VI). The data are the mean ± SD ($n = 3$).

cataract (Fig. 8a & b) due to decreased levels of sorbitol and fructose (Fig. 9a & b) in STZ induced diabetic rat lens, and were compared with two known ARI inhibitors as controls Sorbinil (Group-V) and Fidarestat (Group-VI). From the above *in-vivo* experiments the inhibitory activity of **15e** was demonstrated, it could bring the STZ rats body weights to normal state and it also helped in attenuating the increase in blood glucose levels. In similar to two well-known proven ARI inhibitors, **15e** could also delay the progression of cataract in STZ induced rats.

3. Conclusion

In this study, we have described the design, synthesis, biological activities of the compounds, and protein-ligand interactions of novel series of *N*-(imidazole)-2*H*-chromene-3-carboxamide analogs (**13a**–**j**, **14a**–**d** & **15a**–**f**). Molecular docking studies gave an idea about the binding of these inhibitors, which in turn helped us to understand the interactions of chromene, imidazole and phenyl

Table 3
Effect of **15e** compound in STZ induced diabetic rats with reference to AR activity.

Groups	Parameter	Aldose reductase activity
(Group-I)	Control (uninduced)	34.2 ± 2.50
(Group-II)	Diabetic control	44.66 ± 2.70[a]
(Group-III, 5 μM)	Diabetic+**15e** compound	41.26 ± 1.94[a]
(Group-IV, 50 μM)	Diabetic+**15e** compound	39.54 ± 0.53[b]
(Group –V, 50 μM)	Diabetic + Sorbinil	38.95 ± 1.00[b]
(Group –VI, 50 μM)	Diabetic + Fidarestat	36.28 ± 2.14[b]

The data are the mean ± SD ($n = 3$). SD: Standard deviation.
Aldose reductase activity.
[a] Statistically significant from Group-I (analyzed by ANOVA: $p \leq 0.05$).
[b] Statistically not significant from Group-I (analyzed by ANOVA: $p \leq 0.05$).

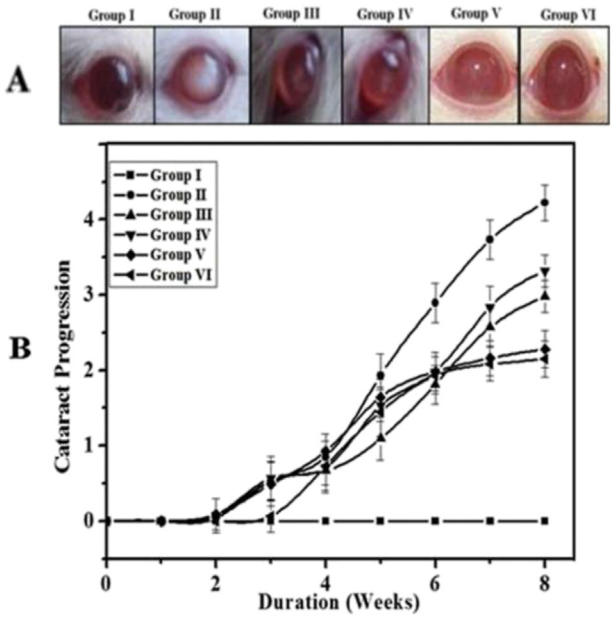

Fig. 8. a & b: Delayed diabetic cataract progression of **15e**. (A) Photographs of lenses from each group at the end of 12 weeks and grading of cataract progression were performed by slit-lamp examination on a weekly basis. In Group I – control uninduced rats, Group –II to VI all were STZ induced rats, Group II diabetic rats were not supplemented with any inhibitory compounds, Group III & IV supplemented with 15e with the concentration of 5 μM & 50 μM, respectively. In the groups V & VI, supplemented with Sorbinil and Fidarestat with 50 μM each, respectively. (B) Cataract formation was scored biweekly according to the following classification: clear normal lens (0), peripheral vesicles (1), peripheral vesicles and cortical opacities (2), diffuse central opacities (3) and mature cataract (4). The data are the mean ± SD ($n = 3$).

rings with ALR2 and ALR1. Among the several promising compounds described here, methoxy group on chromene nucleus, 4-chlorophenyl on imidazole and with pyrrolidine-2-yl spacer derivative (**15e)** emerged for the excellent ALR2 inhibitory activity. In conclusion, the results of the present study indicate that **15e** inhibits ALR2 and ALR1with better selectivity index for ALR2. All the analogs were evaluated for their competent biological assays and **15e** ability to delay progression of cataract in STZ rats. The **15e** compound also shown better Physico-chemical and drug-likeness properties in our *in-silico* analysis. Thus, data also suggest that **15e** might aid in guiding the development of highly specific ALR2 inhibitors without any side effects.

4. Experimental section

4.1. General experimental methods

Compounds 2*H*-3-chromenecarbonitriles (**2a, b)**, 2*H*-3-chromenecarboxylic acids (**3a, b)** and Ary acyl bromides (**4a-f**) are prepared by a repeated procedure [30]. Unless otherwise specified, all solvents and reagents were obtained from commercial suppliers. Solvents were purified as per the procedures are given in the "*Text book of practical organic chemistry*" by Vogel (6th Edition). All reactions were performed under a nitrogen atmosphere unless otherwise noted. Column chromatography was performed using Merck silica gel 60–120 mesh. ^{1}H NMR spectra were recorded on Bruker spectrometer at 400 MHz spectrometer, ^{13}C NMR spectra were acquired on 100.6 MHz with tetramethylsilane as an internal standard, chemical shift (δ) are reported in ppm (δ) Shift (multiplicity, coupling constant, proton count). Mass spectral analysis was accomplished using electro spray ionization (ESI) techniques.

4.2. General procedure for the synthesis of compounds *6a-e, 7a, b & 8a–c*

A mixture of *N*-Boc-amino acids (**5a-c**, 1.0eq) and triethylamine (2.5eq) in dichloromethane in an ice bath was added appropriate phenacyl bromides (**4a-f**, 1.2eq), after addition the solution stirred overnight at room temperature. The reaction mixture was diluted with chloroform and washed with water and brine solution, successively, and dried over Na_2SO_4, after removal of the solvent under reduced pressure; the residue was washed with pet-ether and dried under vacuum. The residue was dissolved in toluene and treated with ammonium acetate (7.0eq) under a nitrogen atmosphere. The reaction mixture was reflux for 12 h. The reaction mixture was quenched with saturated sodium bicarbonate solution. The product was extracted with ethyl acetate (2 times), and washed with water, followed by brine solution, successively and dried over Na_2SO_4. After removal of the solvent under reduced pressure, the crude product was purified by column chromatography using petroleum ether/ethyl acetate to get desired compounds (**6a-e, 7a, b & 8a–c**).

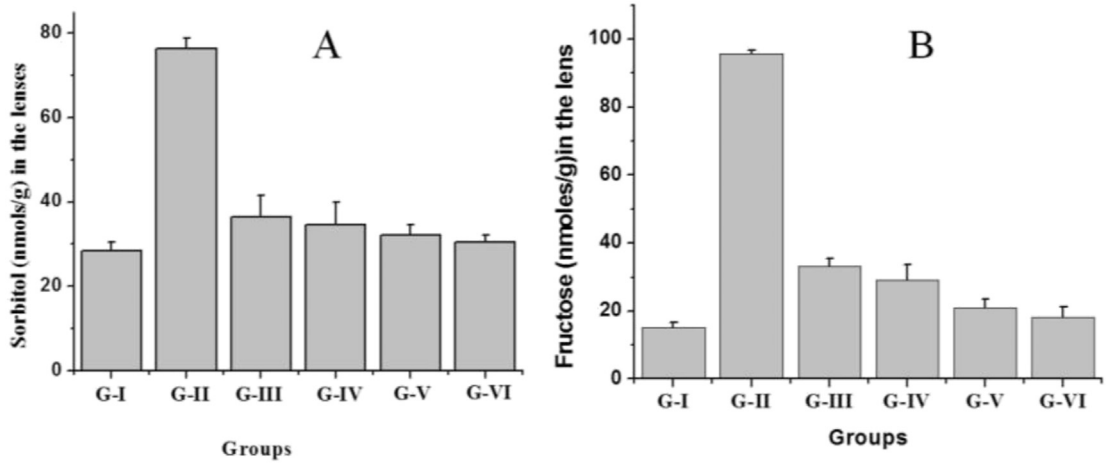

Fig. 9. a & b: Analysis of Sorbitol and Fructose accumulation in diabetic rat lenses. Compound **15e** decreased the accumulation of Sorbitol and Fructose levels in the diabetic rat lens. Eight weeks old rat lens was dissected and used to estimate the Sorbitol and Fructose levels in different groups. In Group I – control uninduced rats, Group –II to VI all were STZ induced rats, Group II diabetic rats were not supplemented with any inhibitory compounds, Group III & IV supplemented with 15e with the concentration of 5 μM & 50 μM, respectively. In the groups V & VI, supplemented with a known ARIs, Sorbinil and Fidarestat with 50 μM each.

*4.2.1. tert-Butyl(5-(phenyl)-1H-imidazol-2-yl)methylcarbamate (**6a**)*

Yield 70%, ^{1}H-NMR (DMSO-d_6) δ: 1.4 (s, 9H, 3xCH_3), 4.19 (d, J = 5.6 Hz, 2H, N–CH_2), 7.16 (t, J = 7.2 Hz, 7.6 Hz, $H_{4'}$), 7.28 (t, J = 4.8 Hz, NH-Boc), 7.33 (t, J = 7.6 Hz, 2H, $H_{3'}$ & $H_{5'}$), 7.47 (s, H_4), 7.73 (d, J = 6.8 Hz, 2H, $H_{2'}$ & $H_{6'}$), 11.87 (s, NH). ^{13}C-NMR (DMSO-d_6) δ: 28.71 (3xCH_3), 38.44 (N–CH_2), 78.5 (^{t}C), 113.15 (C_4), 124.55 ($C_{2'}$ & $C_{6'}$), 126.36 ($C_{4'}$), 128.88 ($C_{3'}$ & $C_{5'}$), 135.35 ($C_{1'}$), 140.13 (C_2), 146.5 (C_5), 156.1 (C=O). MS (ESI, m/z) = 274.05 $[M+H]^+$.

*4.2.2. tert-Butyl(5-(4-chlorophenyl)-1H-imidazol-2-yl) methylcarbamate (**6b**)*

Yield 65%, ^{1}H-NMR (DMSO-d_6) δ: 1.4 (s, 9H, 3xCH_3), 4.18 (d, J = 5.6 Hz, 2H, N–CH_2), 7.28 (t, J = 4.8 Hz, NH-Boc), 7.37 (d, J = 8.4 Hz, 2H, $H_{3'}$ & $H_{5'}$), 7.52 (s, H_4), 7.75 (d, J = 8.4 Hz, 2H, $H_{2'}$ & $H_{6'}$), 11.95 (s, NH). ^{13}C-NMR (DMSO-d_6) δ: 28.7 (3xCH_3), 38.42 (N–CH_2), 78.52 (^{t}C), 113.93 (C_4), 126.19 ($C_{2'}$ & $C_{6'}$), 128.86 ($C_{3'}$ & $C_{5'}$), 130.57 ($C_{1'}$), 134.16 ($C_{4'}$), 137.81 (C_2), 146.78 (C_5), 156.1 (C=O). MS (ESI, m/z) = 307.98 $[M]^+$, 309.95 $[M+2]^+$.

*4.2.3. tert-Butyl(5-(4-bromophenyl)-1H-imidazol-2-yl) methylcarbamate (**6c**)*

Yield 70%, ^{1}H-NMR (DMSO-d_6) δ: 1.4 (s, 9H, 3xCH_3), 4.18 (d, J = 5.6 Hz, 2H, N–CH_2), 7.29 (t, J = 4.8 Hz, NH-Boc), 7.49 (s, H_4), 7.52 (d, J = 7.2 Hz, 2H, $H_{2'}$ & $H_{6'}$), 7.77 (d, J = 8.0 Hz, 2H, $H_{3'}$ & $H_{5'}$), 12.0 (s, NH). ^{13}C-NMR (DMSO-d_6) δ: 28.7 (3xCH_3), 38.47 (N–CH_2), 78.52 (^{t}C), 119.0 (C_4), 126.56 ($C_{4'}$), 130.07 ($C_{2'}$ & $C_{6'}$), 131.7 ($C_{1'}$), 131.76 ($C_{3'}$ & $C_{5'}$), 133.86 (C_2), 146.82 (C_5), 156.1 (C=O). MS (ESI, m/z) = 352.99 $[M+H]^+$, 353.95 $[M + H+2]^+$.

*4.2.4. tert-Butyl(5-(4-fluorophenyl)-1H-imidazol-2-yl) methylcarbamate (**6d**)*

Yield 60%, ^{1}H-NMR (DMSO-d_6) δ: 1.4 (s, 9H, 3xCH_3), 4.19 (d, J = 5.6 Hz, 2H, N–CH_2), 7.28 (t, J = 4.8 Hz, NH-Boc), 7.33 (t, J = 7.6 Hz, 2H, $H_{3'}$ & $H_{5'}$), 7.47 (s, H_4), 7.93 (d, J = 6.8 Hz, 2H, $H_{2'}$ & $H_{6'}$), 11.9 (s, NH). ^{13}C-NMR (DMSO-d_6) δ: 28.71 (3xCH_3), 38.44 (N–CH_2), 78.5 (^{t}C), 112.3 ($C_{3'}$ & $C_{5'}$), 114.5 (C_4), 126.0 ($C_{1'}$), 128.8 ($C_{2'}$ & $C_{6'}$), 138.03 (C_2), 146.1 (C_5), 156.0 (C=O), 159.0 ($C_{4'}$). MS (ESI, m/z) = 278.2 $[M+H]^+$, 300.13 $[M+Na]^+$.

*4.2.5. tert-Butyl(5-(4-methoxyphenyl)-1H-imidazol-2-yl) methylcarbamate (**6e**)*

Yield 55%, ^{1}H-NMR (DMSO-d_6) δ: 1.4 (s, 9H, 3xCH_3), 3.75 (s, 3H, OCH_3), 4.17 (d, J = 5.6 Hz, 2H, N–CH_2), 6.91 (d, J = 8.8 Hz, 2H, $H_{3'}$ & $H_{5'}$), 7.26 (t, J = 5.6 Hz, NH-Boc), 7.31 (s, H_4), 7.64 (d, J = 8.8 Hz, 2H, $H_{2'}$ & $H_{6'}$), 11.9 (s, NH). ^{13}C-NMR (DMSO-d_6) δ: 28.7 (3xCH_3), 38.42 (N–CH_2), 55.48 (OCH_3), 78.48 (^{t}C), 111.28 ($C_{3'}$ & $C_{5'}$), 114.35 (C_4), 125.81($C_{1'}$), 128.88 ($C_{2'}$ & $C_{6'}$), 138.03 (C_2), 146.16 (C_5), 156.1 (C=O), 158.18 ($C_{4'}$). MS (ESI, m/z) = 303.98 [M+H]+, 326.0 $[M+Na]^+$.

*4.2.6. tert-Butyl-(S)-2-methyl-1-(5-phenyl-1H-imidazol-2-yl) propylcarbamate (**7a**)*

Yield 67%, ^{1}H-NMR ($CDCl_3$) δ: 0.76 (d, J = 6.8 Hz, 3H, CH_3), 0.9 (d, J = 6.4 Hz, 3H, CH_3), 1.39 (s, 9H, 3xCH_3), 2.08 (m, CH), 4.41 (t, J = 8.4 Hz, N–CH), 6.98 (d, J = 9.2 Hz, NH-Boc), 7.17 (t, J = 7.2 Hz, $H_{4'}$), 7.33 (t, J = 7.2 Hz, 2H, $H_{3'}$ & $H_{5'}$), 7.46 (s, H_4), 7.72 (d, J = 7.6 Hz, 2H, $H_{2'}$ & $H_{6'}$), 11.83 (s, NH). ^{13}C-NMR (DMSO-d_6) δ: 19.29 (CH_3), 19.72 (CH_3), 28.62 (3xCH_3), 32.98 ($C(CH_3)_2$), 55.15 (N–C), 78.42 ($C(CH_3)_3$), 113.56 (C_4), 124.58 ($C_{2'}$ & $C_{6'}$), 126.41 ($C_{4'}$), 128.92 ($C_{3'}$ & $C_{5'}$), 129.73 ($C_{1'}$), 144.02 (C_5), 149.23 (C_2), 155.71 (C=O). MS (ESI, m/z) = 316.2 $[M+H]^+$.

*4.2.7. tert-Butyl-(S)-2-methyl-1-(5-(4-bromophenyl)-1H-imidazol-2-yl)propylcarbamate (**7b**)*

Yield 60%, ^{1}H-NMR ($CDCl_3$) δ: 0.76 (d, J = 6.8 Hz, 3H, CH_3), 0.89 (d, J = 6.8 Hz, 3H, CH_3), 1.38 (s, 9H, 3xCH_3), 2.07 (m, CH), 4.4 (t, J = 8.4 Hz, N–CH), 6.98 (d, J = 9.2 Hz, NH-Boc), 7.51 (m, 3H, $H_{3'}$, $H_{5'}$ & H_4), 7.7 (d, J = 7.2 Hz, 2H, $H_{2'}$ & $H_{6'}$), 11.86 (s, NH). ^{13}C-NMR (DMSO-d_6) δ: 19.18 (CH_3), 19.72 (CH_3), 28.66 (3xCH_3), 32.88 ($C(CH_3)_2$), 55.13 (N–C), 78.43 ($C(CH_3)_3$), 113.27 (C_4), 118.98 ($C_{4'}$), 126.61 ($C_{2'}$ & $C_{6'}$), 131.74 ($C_{1'}$), 134.76 ($C_{3'}$ & $C_{5'}$), 138.76 (C_5), 149.43 (C_2), 155.72 (C=O). MS (ESI, m/z) = 395.1 $[M+H]^+$, 398.22 $[M + H+2]^+$.

*4.2.8. (S)-tert-butyl 2-(5-phenyl-1H-imidazol-2-yl)pyrrolidine-1-carboxylate (**8a**)*

Yield 66%, ^{1}H-NMR (DMSO-d_6) δ: 1.15 (s, 6H, 2xCH_3), 1.40 (s, 3H, CH_3), 1.90 (m, 3H, H_3, CH_2-4), 2.20 (m, H_3), 3.36 (m, H_5), 3.53 (m, H_5), 4.92 (m, H_2), 7.16 (t, $H_{4''}$), 7.36 (m, $H_{3'}$ & $H_{5''}$), 7.46 (s, $H_{4'}$), 7.72 (d, 2H, $H_{2'}$ & $H_{6''}$), 11.88 (s, NH). ^{13}C-NMR (DMSO-d_6) δ: 23.5 (C_4), 28.3 (3xCH_3), 33.8 (C_3), 46.7 (C_5), 55.7 (C_2), 78.6 (^{t}C), 112.2 ($C_{4'}$), 124.6 ($C_{2'}$ & $C_{6''}$), 126.2 ($C_{4''}$), 128.8 ($C_{3''}$ & $C_{5''}$), 135.6 ($C_{1'''}$), 139.9 ($C_{5'}$), 150.9 ($C_{2'}$), 153.8 (C=O). MS (ESI, m/z) = 341.10 $[M+H]^+$, 336.05 $[M+Na]^+$.

*4.2.9. (S)-tert-butyl-2-(5-(4-chlorophenyl)-1H-imidazol-2-yl) pyrrolidine-1-carboxylate (**8b**)*

Yield 65%, ^{1}H-NMR (DMSO-d_6) δ: 1.14 (s, 6H, 2xCH_3), 1.39 (s, 3H, CH_3), 1.90 (m, 3H, H_3, CH_2-4), 2.17 (m, H_3), 3.36 (m, H_5), 3.52 (m, H_5), 4.79 (m, H_2), 7.36 (t, J = 8.4 Hz, $H_{3''}$ & $H_{5''}$), 7.52 (s, $H_{4'}$), 7.75 (d, J = 8.4 Hz, 2H, $H_{2''}$ & $H_{6''}$), 11.96 (s, NH). ^{13}C-NMR (DMSO-d_6) δ: 23.5 (C_4), 28.3 (3xCH_3), 33.7 (C_3), 46.7 (C_5), 55.7 (C_2), 78.6 (^{t}C), 112.8 ($C_{4'}$), 126.2 ($C_{2''}$ & $C_{6''}$), 128.8 ($C_{3''}$ & $C_{5''}$), 130.4 ($C_{1''}$), 138.8 ($C_{5'}$), 151.1 ($C_{2'}$), 153.8 (C=O). MS (ESI, m/z) = 348.03 $[M]^+$, m/z 350 $[M+2]^+$.

*4.2.10. (S)-tert-butyl-2-(5-(pyridin-3-yl)-1H-imidazol-2-yl) pyrrolidine-1-carboxylate (**8c**)*

Yield 59%, ^{1}H-NMR (DMSO-d_6) δ: 1.15 (s, 6H, 2xCH_3), 1.40 (s, 3H, CH_3), 1.92 (m, 3H, H_3, CH_2-4), 2.20 (m, H_3), 3.36 (m, H_5), 3.53 (m, H_5), 4.80 (m, H_2), 7.33 (dd, J = 7.6, 4.8 Hz, $H_{5''}$), 7.62 (d, J = 9.6 Hz, $H_{4'}$), 8.06 (dd, J = 6.0, 6.4, 2.0, 1.6 Hz, $H_{4''}$), 8.35 (d, J = 3.6 Hz, $C_{6''}$), 8.96 (d, J = 1.2 Hz, $H_{2''}$), 12.0 (d, J = 15.6 Hz, NH). ^{13}C-NMR (DMSO-d_6) δ: 23.5 (C_4), 28.3 (3xCH_3), 33.7 (C_3), 46.7 (C_5), 55.7 (C_2), 78.7 (^{t}C), 113.4 ($C_{4'}$), 124.0 ($C_{5''}$), 131.2 ($C_{3''}$), 131.5 ($C_{4''}$), 136.9 ($C_{5'}$), 146.2 ($C_{6''}$), 147.2 ($C_{2'}$), 151.5 ($C_{2''}$), 153.8 (C=O). MS (ESI, m/z) = 315.03 $[M+H]^+$, 337.05 $[M+Na]^+$.

*4.3. General procedure for the synthesis of compounds **13a–j**, **14a–d** & **15a–f***

Step 1: In a RB flask, compounds (**6a-e, 7a, b** & **8a–c**; 1.0eq) were dissolved in dichloromethane then added TFA. The solution was stirred at room temperature for 6 h. Then the mixture was evaporated to remove the excess of TFA under reduced pressure to obtain the corresponding amines (**9a–e, 10a, b** & **11a–c**).

Step 2: Substituted chromene-3-carboxylic acids (**3a, b**) was carefully added to $SOCl_2$ (5 vol) in a round bottom flask, the solution was refluxed for 6 h, cooled and evaporated under reduced pressure to obtain the corresponding acid chlorides (**12a, b**) as a sticky gum.

Step 3: The acid chloride gum (step-2; 1.0eq) was dissolved into dry dichloromethane cooled in ice-bath and the step-1 amines (**9a–e, 10a, b** & **11a–c**) (1.0eq) was slowly added followed by TEA (3.0eq). The resulting mixture was stirred under N_2 atmosphere at rt for 12 h. The reaction mixture was washed with water, brine, and then dried over anhydrous Na_2SO_4. The solvent was evaporated to dryness and the resulted residue was purified by column chromatography using petroleum ether/ethyl acetate to get required compounds (**13a–j, 14a–d** & **15a–f**).

*4.3.1. N-((5-phenyl-1H-imidazol-2-yl)methyl)-2H-chromene-3-carboxamide (**13a**)*

Off white solid, yield 60%, m.p: 138–140 °C. ^{1}H-NMR (DMSO-d_6) δ: 4.46 (d, J = 5.6 Hz, 2H, CH_2), 4.95 (s, 2H, OCH_2), 6.86 (d, J = 7.6 Hz, H_8), 6.96 (t, J = 7.2 Hz, H_6), 7.2 (m, 4H, H_7, $H_{5'}$ & $H_{4'}$), 7.36 (m, 3H, $H_{3''}$, $H_{4''}$ & $H_{5''}$), 7.5 (s, H_4), 7.74 (d, J = 7.2 Hz, 2H, $H_{2'}$ & $H_{6''}$), 8.81 (t, J = 5.2 Hz, NH–C=O), 12.0 (s, NH). ^{13}C-NMR (DMSO-d_6) δ: 37.24 (N–CH_2), 64.9 (C_2), 116.11 (C_8 & C_{4a}), 121.72$C_{4'}$), 122.29 (C_6), 124.61 (C_5), 126.49 ($C_{2''}$ & $C_{6''}$), 126.98 ($C_{4''}$), 127.77 ($C_{3''}$ & $C_{5''}$), 128.88 (C_7), 128.94 ($C_{1''}$), 131.5 (C_3), 136.0 (C_4 & $C_{2'}$), 146.01 (C_5), 154.58 (C_{8a}), 164.84 (C=O). MS (ESI, m/z) = 332.1 $[M+H]^+$.

*4.3.2. N-((5-(4-Chlorophenyl)-1H-imidazol-2-yl)methyl)-2H-chromene-3-carboxamide (**13b**)*

Light yellow solid, yield 60%, m.p: 150–155 °C. ^{1}H-NMR (DMSO-d_6) δ: 4.42 (d, J = 5.6 Hz, 2H, CH_2–N), 4.91 (s, 2H, OCH_2), 6.81 (d, J = 7.6 Hz, H_8), 7.15 (m, 3H, $H_{4'}$, H_5 & H_6), 7.2 (t, J = 7.4 Hz, H_7), 7.38 (d, J = 7.2 Hz, 2H, $H_{3''}$ & $H_{5''}$), 7.51 (s, H_4), 7.7 (d, J = 8.4 Hz, 2H, $H_{2''}$ & $H_{6''}$), 8.78 (t, J = 5.6, 5.2 Hz, NH–C=O), 12.0 (s, NH). ^{13}C-NMR (DMSO-d_6) δ: 37.2 (CH_2–N), 64.7 (C_2), 113.8 (C_8), 114.8 (C_{4a}), 120.6 ($C_{4'}$), 122.0 (C_6), 126.2 (C_6), 126.4 ($C_{2''}$ & $C_{6''}$), 127.0 ($C_{3''}$ & $C_{5''}$), 127.1 (C_7), 127.9 ($C_{1''}$), 128.8 ($C_{4''}$), 130.6, (C_3) 134.3 (C_4), 138.9 ($C_{2'}$), 143.5 ($C_{5'}$), 146.1 (C_{8a}), 148.1 (C_8), 164.8 (C=O). MS (ESI) m/z = 366.1 $[M+H]^+$.

*4.3.3. N-((5-(4-bromophenyl)-1H-imidazol-2-yl)methyl)-2H-chromene-3-carboxamide (**13c**)*

Off white solid, yield 70%, m.p: 140–145 °C. ^{1}H-NMR (DMSO-d_6) δ: 4.45 (d, J = 5.6 Hz, 2H, CH_2–N), 5.07 (s, 2H, OCH_2), 6.86 (d, J = 7.6 Hz, H_8), 6.96 (t, J = 7.6, 7.2 Hz, H_6), 7.22 (m, 3H, H_5, H_7 & $H_{4'}$), 7.53 (d, J = 8.4 Hz, 2H, $H_{3''}$ & $H_{5''}$), 7.63 (s, H_4), 7.7 (d, J = 8.4 Hz, 2H, $H_{2''}$ & $H_{6''}$), 10.04 (t, J = 5.6, 4.4 Hz, NH–C=O), 12.24 (s, NH). ^{13}C-NMR (DMSO-d_6) δ: 37.7 (C–NH), 64.8 (C_2), 113.9 (C_8), 114.8 (C_{4a}), 119.1 ($C_{4'}$), 120.9 ($C_{4''}$), 126.6 (C_5), 127.1 (C_7), 127.9 ($C_{2''}$ & $C_{6''}$), 131.8 ($C_{3''}$ & $C_{5''}$), 133.7 (C_3 & $C_{1''}$), 139.0 ($C_{2'}$), 143.5 ($C_{5'}$), 148.1 (C_{8a}), 164.8 (C=O). MS (ESI) m/z = 411.0 $[M+H]^+$, 413.2 $[M + H+2]^+$.

*4.3.4. N-(5-(4-fluorophenyl)-1H-imidazol-2-yl)methyl)-2H-chromene-3-carboxamide (**13d**)*

Brown solid, yield 55%, m.p: 150–154 °C. ^{1}H-NMR (DMSO-d_6) δ: 4.12 (d, J = 5.6 Hz, 2H, CH_2), 4.62 (s, 2H, OCH_2), 6.69 (d, J = 8.0 Hz, H_8), 7.08 (s, $H_{4'}$), 6.97 (t, J = 7.6 Hz, H_6), 7.27 (m, 4H, H_5, H_7, $H_{3''}$ & $H_{5''}$), 7.66 (s, H_4), 7.87 (m, 2H, $H_{2''}$ & $H_{6''}$), 9.6 (t, J = 2.0 Hz, NH–C=O), 11.83 (s, NH). ^{13}C-NMR (DMSO-d_6) δ: 36.29 (N–CH_2), 64.73 (C_2), 116.17 (C_8 & C_{4a}), 117.67 ($C_{3''}$ & $C_{5''}$), 119.85 ($C_{4'}$), 122.38 (C_6), 126.63 ($C_{1''}$), 126.55 (C_5), 127.29 (C_7), 127.92 ($C_{2''}$ & $C_{6''}$), 129.02 (C_3), 129.78 (C_4), 141.84 ($C_{2'}$), 144.15 ($C_{5'}$), 154.78 (C_{8a}), 157.38 ($C_{4''}$), 165.97 (C=O). 350.0 $[M+H]^+$.

*4.3.5. N-((5-(4-methoxyphenyl)-1H-imidazol-2-yl)methyl)-2H-chromene-3-carboxamide (**13e**)*

Yellow solid, yield 50%, m.p: 160–167 °C. ^{1}H-NMR (DMSO-d_6) δ: 3.77 9s, OCH_3), 4.42 (d, J = 5.6 Hz, CH_2), 4.91 (s, OCH_2), 6.85 (d, J = 7.6 Hz, H_8), 6.91 (m, 3H, H_6, $H_{3''}$ & $H_{5''}$), 7.35 (d, J = 7.2 Hz, $H_{2''}$ & $H_{6''}$), 7.5 (s, H_4), 8.79 (t, J = 5.6, 5.2 Hz, NH–C=O), 11.85)s, NH). ^{13}C-NMR (DMSO-d_6) δ: 36.0 (N–CH_2), 55.48 (OCH_3), 64.7 (C_2), 114.35 ($C_{3''}$ & $C_{5''}$), 116.2 (C_{4a} & C_8), 121.7 ($C_{4'}$), 122.2 (C_6), 124.6 ($C_{1''}$), 126.5 (C_5), 127.2 ($C_{2''}$ & $C_{6''}$), 127.9 (C_7), 129.2 (C_3), 136.5 (C_4), 138.0 ($C_{2'}$), 141.5 ($C_{5'}$), 154.7 (C_{8a}), 158.1 ($C_{4''}$), 165.0 (C=O). 362.15 $[M+H]^+$.

*4.3.6. 8-Methoxy-N-((5-phenyl-1H-imidazol-2-yl)methyl)-2H-chromene-3-carboxamide (**13f**)*

Light yellow solid, yield 65%, m.p: 110–115 °C. ^{1}H-NMR (DMSO-d_6) δ: 3.76 (s, 3H, OCH_3), 4.63 (d, J = 5.6 Hz, 2H, CH_2–N), 4.93 (s, 2H, OCH_2), 6.92 (m, 3H, H_7, H_6 & H_5), 7.36 (m, 4H, $H_{4'}$, $H_{3''}$, $H_{5''}$ & $H_{4''}$), 7.82 (m, 3H, $H_{4'}$, $H_{2''}$ & $H_{6''}$), 9.04 (s, NH–C=O), 12.1 (s, NH). ^{13}C-NMR (DMSO-d_6) δ: 35.9 (C–NH), 56.1 (OCH_3), 64.6 (C_2), 115.0 (C_7), 115.4 (C_{4a}), 120.7 ($C_{4'}$ & C_5), 122.3 (C_6), 125.3 ($C_{2''}$& $C_{6''}$), 128.4 ($C_{3''}$ & $C_{5''}$), 128.6 ($C_{1''}$), 129.4 (C_3), 134.9 (C_4 & $C_{2'}$), 143.5 ($C_{5'}$), 146.2 (C_{8a}), 148.1 (C_8), 165.2 (C=O). MS (ESI) m/z = 362.15 $[M+H]^+$.

*4.3.7. N-(5-(4-Chlorophenyl)-1H-imidazol-2-yl)methyl)-8-methoxy-2H-chromene-3-carboxamide (**13g**)*

Off white solid, yield 68%, m.p: 180–185 °C. ^{1}H-NMR (DMSO-d_6) δ: 3.79 (s, 3H, OCH_3), 4.43 (d, J = 5.6 Hz, 2H, CH_2–N), 4.87 (s, 2H, OCH_2), 6.82 (d, J = 7.6 Hz, H_7), 6.9 (t, J = 8.0, 7.6 Hz, H_6), 6.98 (d, J = 6.8 Hz, H_5), 7.32 (s, $H_{4'}$), 7.37 (d, J = 8.4 Hz, 2H, $H_{3''}$ & $H_{5''}$), 7.58 (s, H_4), 7.77 (d, J = 8.4 Hz, 2H, $H_{2''}$ & $H_{6''}$), 8.77 (t, J = 4.8 Hz, NH–C=O), 12.0 (s, NH). ^{13}C-NMR (DMSO-d_6) δ: 37.2 (CH_2–N), 56.1 (OCH_3), 64.8 (C_2), 113.8 (C_7), 114.8 (C_{4a}), 120.6 ($C_{4'}$), 122.0 (C_5), 122.4 (C_6), 126.2 ($C_{2''}$ & $C_{6''}$), 127.0 ($C_{3''}$ & $C_{5''}$), 127.9 ($C_{1''}$), 128.8 ($C_{4''}$), 130.5, (C_3) 134.3 (C_4), 138.9 ($C_{2'}$), 143.5 ($C_{5'}$), 148.1 (C_8), 164.8 (C=O). MS (ESI) m/z = 396.15 $[M+H]^+$.

*4.3.8. N-(5-(4-bromophenyl)-1H-imidazol-2-yl)methyl)-8-methoxy-2H-chromene-3-carboxamide (**13h**)*

White solid, yield 60%, m.p: 241–245 °C. ^{1}H-NMR (DMSO-d_6) δ: 3.76 (s, 3H, OCH_3), 4.43 (d, J = 5.6 Hz, 2H, CH_2–N), 4.93 (s, 2H, OCH_2), 6.83 (d, J = 6.8 Hz, H_7), 6.91 (t, J = 7.6, 8.0 Hz, H_6), 6.97 (d, J = 8.0 Hz, H_5), 7.23 (s, $H_{4'}$), 7.44 (d, J = 8.0 Hz, 2H, $H_{3''}$ & $H_{5''}$), 7.61 (s, H_4), 7.72 (d, J = 7.2 Hz, 2H, $H_{2''}$ & $H_{6''}$), 8.25 (t, J = 8.0 Hz, NH–C=O), 12.12 (s, NH). ^{13}C-NMR (DMSO-d_6) δ: 37.2 (C–NH), 56.1 (OCH_3), 64.7 (C_2), 113.9 (C_7), 114.8 (C_{4a}), 120.6 ($C_{4''}$), 121.9 (C_5), 122.4 (C_6), 126.6 ($C_{4''}$), 127.0 ($C_{2''}$ & $C_{6''}$), 127.9 ($C_{1''}$), 131.8 ($C_{3''}$ & $C_{5''}$), 133.3 (C_3), 134.6 (C_4 & $C_{2'}$), 143.5 ($C_{5'}$), 146.2 (C_{8a}), 148.0 (C_8),164.8 (C=O). MS (ESI) m/z = 440.05 $[M+H]^+$, 442.05 $[M + H+2]^+$.

*4.3.9. N-(5-(4-fluorophenyl)-1H-imidazol-2-yl)methyl)-8-methoxy-2H-chromene-3-carboxamide (**13i**)*

Off white solid, yield 45%, m.p: 160–165 °C. ^{1}H-NMR (DMSO-d_6) δ: 3.76 (s, 3H, OCH_3), 4.6 (s, 2H, CH_2–N), 4.92 (s, 2H, OCH_2), 6.83 (d, J = 6.8 Hz, H_7), 6.92 (t, J = 8.4, 6.8 Hz, H_6), 7.0 (d, J = 7.2 Hz, H_5), 7.12 (s, $H_{4'}$), 7.27 (m, 2H, $H_{3''}$ & $H_{5''}$), 7.84 (m, 3H, H_4, $H_{2''}$ & $H_{6''}$), 9.02 (s, NH–C=O), 12.0 (s, NH). ^{13}C-NMR (DMSO-d_6) δ: 35.9 (C–NH), 56.1 (OCH_3), 64.6 (C_2), 115.0 (C_7), 115.4 (C_{4a}), 117.7 ($C_{3''}$ & $C_{5''}$), 120.6 (C_5 & $C_{4'}$), 122.05 (C_6), 125.3 ($C_{1''}$), 128.6 ($C_{2''}$ & $C_{6''}$), 129.5 (C_3), 134.9 (C_4 & $C_{2'}$), 143.5 ($C_{5'}$), 146.2 (C_{8a}), 148.0 (C_8), 159.14 ($C_{4''}$), 165.2 (C=O). MS (ESI) m/z = 381.3 $[M+H]^+$.

*4.3.10. 8-Methoxy-N-((5-(4-methoxyphenyl)-1H-imidazol-2-yl) methyl)-2H-chromene-3 carboxamide (**13j**)*

Off white solid, yield 45%, m.p: 145–150 °C. ^{1}H-NMR (DMSO-d_6) δ: 3.74 (s, 3H, OCH_3), 3.76 (s, 3H, OCH_3), 4.41 (d, J = 5.6 Hz, 2H, CH_2–N), 4.91 (s, 2H, OCH_2), 6.81 (d, J = 7.6 Hz, H_7), 6.9 (m, 3H, H_6, H_5 & $H_{4'}$), 6.98 (d, J = 7.2 Hz, 2H, $H_{3''}$ & $H_{5''}$), 7.33 (s, H_4), 7.66 (d, J = 8.8 Hz, 2H, $H_{2''}$ & $H_{6''}$), 8.78 (t, J = 5.6, 5.2 Hz, NH–C=O), 11.85 (s, NH).). ^{13}C-NMR (DMSO-d_6) δ: 35.8 (CH_2–N), 56.2 (OCH_3), 64.4 (C_2), 115.0 (C_7), 115.4 ($C_{3''}$ & $C_{5''}$), 116.5 (C_{4a}), 120.0 (C_5), 120.6 ($C_{4'}$), 122.5 (C_6), 124.5 ($C_{1''}$), 128.6 ($C_{2''}$ & $C_{6''}$), 129.4 (C_3), 134.9 (C_4), 138.5 ($C_{2'}$), 143.5 ($C_{5'}$), 146.2 (C_{8a}), 148.0 (C_8), 159.5 ($C_{4''}$), 165.2 (C=O). MS (ESI) m/z = 392.15 $[M+H]^+$.

*4.3.11. N-(S)-2-Methyl-1-(5-phenyl-1H-imidazol-2-yl)propyl)-2H-chromene-3- carboxamide (**14a**)*

Light green solid, yield 55%, m.p: 118–120 °C. ^{1}H-NMR (DMSO-d_6) δ: 0.81 (d, J = 6.8 Hz, 3H, CH_3), 0.98 (d, J = 6.8 Hz, 3H, CH_3), 2.3 (m, CH-(CH_3)$_2$), 4.9 (m, 3H, OCH_2 & CH–N), 6.85 (d, J = 8.0 Hz, H_8), 6.96 (t, J = 7.6, 6.8 Hz, H_6), 7.17 (t, J = 7.2 Hz, H_7), 7.23 (m, 3H, $H_{4''}$, $H_{4'}$ & H_5), 7.34 (t, J = 7.6 Hz, 2H, $H_{3''}$ & $H_{5''}$), 7.42 (s, H_4), 7.74 (d, J = 6.8 Hz, 2H, $H_{2''}$ & $H_{6''}$), 8.45 (d, J = 8.8 Hz, NH–C=O), 12.0 (s,

NH). ^{13}C-NMR (DMSO-d_6) δ: 19.7 (CH_3), 20.07 (CH_3), 32.33 (C-(CH_3)$_2$), 53.58 (C–NH), 64.94 (C_2), 116.11 (C_{4a}), 121.75 ($C_{4'}$), 122.28 (C_6), 124.63 ($C_{2''}$ & $C_{6''}$), 126.92 ($C_{4''}$), 127.59 (C_7), 128.87 ($C_{3''}$ & $C_{5''}$), 128.93 ($C_{1''}$), 131.44 (C_3), 134.61 (C_4), 142.92 ($C_{5'}$), 148.87 ($C_{2'}$), 154.61 (C_{8a}), 164.61 (C=O). MS (ESI) m/z = 374.2 $[M+H]^+$.

4.3.12. N-(S)-1-(5-(4-bromophenyl)-1H-imidazol-2-yl)-2-methylpropyl)-2H-chromene-3-carboxamide (**14b**)

White solid, yield 55%, m.p: 140–145 °C. ^{1}H-NMR (DMSO-d_6) δ: 0.82 (d, J = 6.8 Hz, 3H, CH_3), 0.98 (d, J = 6.8 Hz, 3H. CH_3), 2.3 (m, CH-(CH_3)$_2$), 4.97 (m, 3H, OCH_2 & CH–N), 6.85 (d, J = 8.0 Hz, H_8), 6.96 (t, J = 7.6, 6.4 Hz, H_6), 7.23 (m, 2H, H_5 & H_7), 7.42 (s, $H_{4'}$), 7.51 (d, J = 8.0 Hz, 2H, $H_{3''}$ & $H_{5''}$), 7.58 (s, H_4), 7.72 (d, J = 7.6 Hz, 2H, $H_{2''}$ & $H_{6''}$), 8.45 (d, J = 8.8 Hz, NH–C=O), 12.04 (s, NH). ^{13}C-NMR (DMSO-d_6) δ: 19.6 (CH_3), 20.1 (CH_3), 32.2 (C-(CH_3), 53.5 (C–NH), 64.9 (C_2), 113.3 (C_8), 116.1 (C_{4a}), 121.7 (C_6), 122.3 ($C_{4''}$), 126.7 (C_5), 126.9 (C_7), 127.6 ($C_{2''}$ & $C_{6''}$), 128.8 ($C_{1''}$), 131.4 ($C_{3''}$ & $C_{5''}$), 131.7 (C_3), 134.7 (C_4), 138.9 ($C_{5'}$), 149.1 ($C_{2'}$), 154.6 (C_{8a}), 164.6 (C=O). MS (ESI) m/z = 452.1 $[M+H]^+$, 454.1 $[M+H+2]^+$.

4.3.13. 8-Methoxy-N-(S)-2-methyl-1-(5-phenyl-1H-imidazol-2-yl) propyl)-2H-chromene-3-carboxamide (**14c**)

Off white solid, yield 50%, m.p: 155–157 °C. ^{1}H-NMR (DMSO-d_6) δ: 0.82 (d, J = 6.8 Hz, 3H, CH_3), 0.98 (d, J = 6.8 Hz, 3H, CH_3), 2.33 (m, CH-(CH_3)$_2$), 3.75 (s, 3H, OCH_3), 4.9 (m, 3H, OCH_2 & CH–N), 6.85 ((d, J = 6.4 Hz, H_7), 6.91 (t, J = 7.6, 8.0 Hz, H_6), 6.98 (d, J = 6.8 Hz, H_5), 7.17 (t, J = 7.2, 6.8 Hz, $H_{4''}$), 7.34 (t, J = 7.2, 7.6 Hz, 2H, $H_{3''}$ & $H_{5''}$), 7.41 (s, $H_{4'}$), 7.48 (s, H_4), 7.74 (d, J = 7.2 Hz, 2H, $H_{2''}$ & $H_{6''}$), 8.46 (d, J = 8.8 Hz, NH–C=O), 12.0 (s, NH). ^{13}C-NMR: 19.7 (CH_3), 20.0 (CH_3), 32.3 (C-(CH_3)$_2$), 55.6 (OCH_3), 56.1 (C–NH), 64.8 (C_2), 114.7 (C_7), 120.6 (C_{4a}), 121.9 (C_5 & $C_{4'}$), 122.4 (C_6), 124.6 ($C_{2''}$ & $C_{6''}$), 126.9 ($C_{3''}$ & $C_{5''}$), 126.4 ($C_{4''}$), 127.7 ($C_{1''}$), 128.9 (C_3 & C_4), 143.5 ($C_{5'}$), 148.0 (C_{8a}), 148.9 (C_8 & $C_{2'}$), 164.6 (C=O). MS (ESI) m/z = 404.2 $[M+H]^+$.

4.3.14. N-(S)-1-(5-(4-bromophenyl)-1H-imidazol-2-yl)-2-methylpropyl)-8-methoxy-2H-chromene-3-carboxamide (**14d**)

Off white solid, yield 50%, m.p: 185–187 °C. ^{1}H-NMR (DMSO-d_6) δ: 0.82 (d, J = 6.4 Hz, 3H, CH_3), 0.97 (d, J = 6.4 Hz, 3H, CH_3), 2.3 (m, CH-(CH_3)$_2$), 3.75 (s, 3H, OCH_3), 4.86 (m, 3H, OCH_2 & CH–N), 6.84 (d, J = 6.8 Hz, H_7), 6.91 (t, J = 7.6, 8.0 Hz, H_6), 6.98 (d, J = 8.0 Hz, H_5), 7.4 (s, $H_{4'}$), 7.52 (d, J = 8.0 Hz, 2H, $H_{3''}$ & $H_{5''}$), 7.56 (s, H_4), 7.7 (d, J = 7.2 Hz, 2H, $H_{2''}$ & $H_{6''}$), 8.45 (d, J = 8.4 Hz, NH–C=O), 120.3 (s, NH). ^{13}C-NMR (DMSO-d_6) δ: 19.9 (CH_3), 20.1 (CH_3), 32.3 (C-(CH_3)$_2$), 53.5 (OCH_3), 56.1 (C–NH), 64.7 (C_2), 114.8 (C_7), 119.2 (C_{4a}), 120.6 ($C_{4'}$), 122.0 (C_5), 122.3 ($C_{4''}$), 122.7 (C_6), 124.1 ($C_{2''}$ & $C_{6''}$), 126.7 ($C_{1''}$), 127.9 ($C_{3''}$ & $C_{5''}$), 131.8 (C_3), 135.2 (C_4), 143.5 ($C_{5'}$), 148.0 (C_{8a} & $C_{2'}$), 149.2 (C_8), 164.7 (C=O). MS (ESI) m/z = 484.1 $[M+H]^+$.

4.3.15. (2H-chromen-3-yl)(S)-2-(5-phenyl-1H-imidazol-2-yl) pyrrolidin-1-yl)methanone (**15a**)

Light green solid, yield 50%, m.p: 130–132 °C. ^{1}H-NMR (DMSO-d_6) δ: 2.1 (m, 4H, CH_2-3′, CH_2-4′), 3.8 (m, 2H, CH_2-5′), 4.83 (s, 2H, OCH_2), 5.15 (m, $H_{2'}$), 6.86 (d, J = 1.2 Hz, H_8), 6.96 (d, J = 2.8 Hz, H_5), 7.01 (s, $H_{4''}$), 7.24 (m, 3H, H_6 & H_7), 7.34 (m, 3H, $H_{3'''}$, $H_{4'''}$ & $H_{5'''}$), 7.47 (s, H_4), 12.14 (s, NH). ^{13}C-NMR (DMSO-d_6) δ: 25.32 ($C_{4'}$), 31.83 ($C_{3'}$), 49.83 ($C_{5'}$), 55.53 ($C_{2'}$), 65.47 (C_2), 116.05 (C_8 & C_{4a}), 121.86 ($C_{4'}$), 122.2, 124.65 (C_5), 126.47 ($C_{2'''}$ & $C_{6'''}$), 128.89 (C_7), 128.99 ($C_{3'''}$ & $C_{5'''}$), 131.95 ($C_{1'''}$), 132.01(C_3), 135.0 (C_4), 142.87 ($C_{5''}$), 149.73 ($C_{2''}$), 160.5 (C=O). MS (ESI) m/z = 372.15 $[M+H]^+$.

4.3.16. (S)-2-(5-(4-Chlorophenyl)-1H-imidazol-2-yl)pyrrolidin-1-yl)(2H-chromen-3l)methanone (**15b**)

Light green solid, yield 50%, m.p: 140–142 °C. ^{1}H-NMR (DMSO-d_6) δ: 1.92 (m, 4H, CH_2-3′, CH_2-4′), 3.85 (m, 2H, CH_2-5′), 5.0 (m, 3H, OCH_2 & $H_{2'}$), 6.85 (d, J = 8.0 Hz, 2H, H_8 & H_5), 7.2 (m, 3H, H_6, H_7 & $H_{4''}$), 7.38 (d, J = 8.0 Hz, 2H, $H_{3'''}$ & $H_{5'''}$), 7.53 (s, H_4), 7.75 (m, 2H, $H_{2'''}$ & $H_{6'''}$), 12.15 (s, NH). ^{13}C-NMR (DMSO-d_6) δ: 25.32 ($C_{4'}$), 31.83 ($C_{3'}$), 49.59 ($C_{5'}$), 55.56 ($C_{2'}$), 65.47 (C_2), 116.05 (C_8 & C_{4a}), 121.88 ($C_{4'}$), 122.17 (C_6), 126.12 (C_5), 128.15 ($C_{2''}$ & $C_{6'''}$), 128.85 (C_7), 129.36 ($C_{3'''}$ & $C_{5'''}$), 130.59 ($C_{1'''}$), 131.12 ($C_{4'''}$ & C_3), 134.0 (C_4), 140.0 ($C_{5''}$), 149.93 ($C_{2''}$), 154.3 (C_{8a}), 166.34 (C=O). MS (ESI) m/z = 406.15 $[M+H]^+$.

4.3.17. (2H-chromen-3-yl)(S)-2-(5-(pyridin-3-yl)-1H-imidazol-2-yl)pyrrolidin-1-yl)methanone (**15c**)

Brown solid, yield 40%, m.p: 122–123 °C. ^{1}H-NMR (DMSO-d_6) δ: 2.0 (m, 3H, $H_{3'}$, CH_2-4′), 2.28 (m, $H_{3'}$), 3.8 (m, 2H, CH_2-5′), 5.0 (m, 3H, OCH_2 & $H_{2'}$), 6.9 (m, 2H, H_8 & H_6), 7.2 (m, 3H, H_5, H_7 & $H_{4''}$), 7.36 (s, H_4), 7.65 (m, $H_{4'''}$), 8.08 (m, $H_{5'''}$), 8.38 (m, $H_{6'''}$), 8.96 (s, $H_{2'''}$), 12.4 (s, NH). ^{13}C-NMR (DMSO-d_6) δ: 23.49 ($C_{4'}$), 31.8 (C3′), 33.76 (C5′), 55.54 (C2′), 65.77 (C2), 114.2 (C_8), 116.06 (C_{4a}), 119.1 ($C_{4''}$), 122.18 (C_6), 124.67 ($C_{5'''}$), 126.4 (C_5), 128.74 (C_7), 131.67 ($C_{1'''}$), 134.1 ($C_{6'''}$), 136.6 (C_4), 140.5 ($C_{5''}$), 146.66 ($C_{4'''}$), 147.4 ($C_{2'''}$ & $C_{2''}$), 157.72 (C_{8a}), 164.11 (C=O). MS (ESI) m/z = 373.2 $[M+H]^+$.

4.3.18. (8-methoxy-2H-chromen-3-yl)(S)-2-(5-phenyl-1H-imidazol-2-yl)pyrrolidin-1-yl) methanone (**15d**)

Brown solid, yield 45%, m.p: 122–126 °C. ^{1}H-NMR (DMSO-d_6) δ: 2.1 (m, 4H, CH_2-3′, CH_2-4′), 3.6 (m, 2H, CH_2-5′), 3.8 (s, 3H, OCH_3), 4.92 (s, 2H, OCH_2), 5.23 (m, $H_{2'}$), 6.83 (d, J = 8.8 Hz, H_7), 6.93 (t, J = 5.6, 5.6 Hz, H_6), 7.0 (t, J = 8.0, 7.6 Hz, H_5), 7.18 (s, $H_{4'}$), 7.25 (m, 2H, $H_{3''}$ & $H_{5''}$), 7.34 (m, $H_{4''}$), 7.72 (m, 3H, $H_{2''}$, H_4 & $H_{6''}$), 12.1 (s, NH). ^{13}C-NMR (DMSO-d_6) δ: 25.3 ($C_{4'}$), 32.0 ($C_{3'}$), 42.5 ($C_{5'}$), 56.1 (OCH_3), 57.0 ($C_{2'}$), 65.3 (C_2), 114.5 (C_7), 118.5 (C_{4a}), 120.6 ($C_{4'}$), 122.0 (C_5), 122.7 (C_6), 126.9 ($C_{2'''}$ & $C_{6'''}$), 127.6 ($C_{4'''}$), 129.1 ($C_{3'''}$ & $C_{5'''}$), 131.5 (C_3 & $C_{1'''}$), 133.4 (C_4), 142.52 ($C_{5''}$), 147.9 (C_{8a} & $C_{2''}$), 150.0 (C_8), 172.8 (C=O). MS (ESI) m/z = 402.2 $[M+H]^+$.

4.3.19. (S)-2-(5-(4-Chlorophenyl)-1H-imidazol-2-yl)pyrrolidin-1-yl)(8-methoxy-2H-chromen-3-yl)methanone (**15e**)

Light brown solid, yield 50%, m.p: 110–115 °C. ^{1}H-NMR (DMSO-d_6) δ: 2.0 (m, 3H, $H_{3'}$, CH_2-4′), 2.28 (m, $H_{3'}$), 3.76 (m, 4H, OCH_3 & $H_{2'}$), 5.2 (s, 2H, OCH_2), 6.9 (d, J = 8.0 Hz, 2H, H_7 & H_5), 7.2 (m, 2H. H_6 & $H_{4'}$), 7.46 (m, 5H, $H_{2''}$, $H_{3''}$, $H_{5''}$ & $H_{6''}$), 7.75 (s, H_4), 12.08 (s, NH), ^{13}C-NMR (DMSO-d_6) δ: 24.0 ($C_{4'}$), 31.9 ($C_{3'}$), 48.5 ($C_{5'}$), 56.3 (OCH_3), 57.0 ($C_{2'}$), 64.5 (C_2), 115.2 (C_7), 119.8 (C_{4a}), 120.5 ($C_{4'}$), 122.2 (C_5), 122.5 (C_6), 126.3 ($C_{2'''}$ & $C_{6'''}$), 128.8 ($C_{3'''}$ & $C_{5'''}$), 130.6 ($C_{1'''}$), 131.1 (C_3 & $C_{4'''}$), 135.2 (C_4), 142.2 ($C_{5''}$), 145.4 (C_{8a} & $C_{2'}$), 148.2 (C_8), 167.6 (C=O). MS (ESI) m/z = 436.15 $[M+H]^+$.

4.3.20. (8-methoxy-2H-chromen-3-yl)(S)-2-(5-(pyridin-3-yl)-1H-imidazol-2-yl)pyrrolidin-1-yl)methanone (**15f**)

Orange solid, yield 40%, m.p: 138–140 °C. ^{1}H-NMR (DMSO-d_6) δ: 1.92 (m, 3H, $H_{3'}$, CH_2-4′), 2.20 (m, $H_{3'}$), 3.36 (m, $H_{5'}$), 3.53 (m, $H_{5'}$), 3.78 (s, OCH_3), 4.80 (m, $H_{2'}$), 5.19 (s, OCH_2), 6.8 (d, J = 6 Hz, H_7), 6.9 (m, 2H, H_5 & H_6), 7.19 (s, $H_{4''}$), 7.41 (t, J = 4.8, 6.0 Hz, $H_{5'''}$), 7.93 (s, H_4), 8.15 (d, J = 8.0 Hz, $H_{6'''}$), 8.42 (d, J = 3.2 Hz, $H_{4'''}$), 9.03 (s, $H_{2'''}$), 12.82 (s, NH). ^{13}C-NMR (DMSO-d_6): 23.4 ($C_{4'}$), 31.8 ($C_{3'}$), 47.0 ($C_{5'}$), 55.3 (OCH_3), 56.5 ($C_{2'}$), 65.4 (C_2), 114.2 (C_7), 119.0 (C_{4a}), 120.4 ($C_{4'}$), 122.0 (C_5), 122.7 (C_6), 124.6 ($C_{5'''}$), 131.7 ($C_{3'''}$), 134.5 ($C_{6'''}$ & C_3), 136.1 (C_4), 140.5 ($C_{5''}$), 146.1 ($C_{4'''}$ & C_{8a}), 147.4 ($C_{2'''}$), 148.0 ($C_{2''}$ & C_8), 166.1 (C=O), MS (ESI) m/z = 403.2 $[M+H]^+$.

5. Biological assay studies

5.1. Materials

DL-glyceraldehyde, Lithium sulfate, β-mercaptoethanol, Butylated hydroxytoluene, NADPH, Sorbinil, Fidarestat, were procured from Sigma Chemicals (MO, USA). All other chemicals and solvents were of analytical grade and obtained from SRL (Mumbai, India).

5.2. Aldose reductase inhibition

ALR2 activity was performed at 30 °C in a reaction mixture containing 0.25 mL of NADPH (0.10 mM), 0.25 ml of sodium phosphate buffer (0.1 M, pH 6.2), 0.1 mL of enzyme extract, 0.15 mL of deionized water, and 0.25 mL of DL-glyceraldehyde (10 mM) as substrate in a final volume of 1 mL. The reaction mixture, except for DL-glyceraldehyde, was incubated at 30 °C for 10 min. The substrate was then added to start the reaction, which was monitored for 4 min. ALR1 activity assays were performed at 37 °C in a reaction mixture containing 0.25 mL of NADPH (0.12 mM), 0.1 mL of enzyme extract, 0.25 mL of sodium phosphate buffer (0.1 M, pH 7.2), 0.15 mL of deionized water, and 0.25 mL of sodium D-glucuronate (20 mM) as a substrate in a final volume of 1 mL. The reaction mixture, except for sodium D-glucuronate, was incubated at 37 °C for 10 min. The substrate was then added to start the reaction, which was monitored for 4min.

The inhibitory activity of the newly synthesized compounds against ALR2 and ALR1 was assayed by adding 5 mL of the inhibitor solution to the reaction mixture described above. All compounds were dissolved in dimethyl sulfoxide (DMSO) and diluted with deionized H_2O. To correct for the nonenzymatic oxidation of NADPH, the rate of NADPH oxidation in the presence of all the reaction mixture components except the substrate was subtracted from each experimental rate. The inhibitory effect of the synthetic compounds was routinely estimated in a concentration ranges from 1 μM to 50 μM. Most dose-response curves were generated using at least three concentrations of compound with inhibitory activity between 20% and 80%, with three replicates at each concentration. The 95% confidence limits (95% CL) were calculated from t values for $n = 5$, where n is the total number of determinations.

5.3. Molecular docking studies

We docked **20** molecules and conformational searches were performed using version 2015-3 of the Schrodinger. The results are compared with the co-crystal structures (PDB codes: 2FZB, 1Z3N, 2DUX, 1PWM & 1AH0). The PDB ID 1Z3N & 1US0 were used for the docking studies. The protein was prepared by using the prot prep option by treatment like adding hydrogen, adding missing residues, refining the loop with prime and finally minimized by using OPLS 2005 force field. The search grid was generated by picking the co-crystal ligand upto 15 Å search area. The hydroxyl groups of search area were allowed to move.

All the molecules were minimized by using macromodule application. We used 1000 iterations for minimization using OPLS 2005 force field and charges were also added from force field only. All the molecules were docked by using glide SP (standard precision) dock application. We performed flexible docking by allowing ring conformations and nitrogens to move to possible extensions. 10 poses were generated for each ligand. The docking results are sorted out and analyzed based on docking scores and their interactions with active site residues.

The molecular alignment was performed with the align program (PyMol). The highest active compound **15e** was used as the template and all the other compounds were aligned to the common core. The common structure and the aligned inhibitors are displayed in Fig. 5a&b, respectively.

5.4. Animal experiment

Three month old male SD (Sprague Dawley) rats with an average body weight of 200 ± 6 g were used in this study. All the animals were fed with AIN-93 diet ad libitum. The control group rats (Group-I, n = 12) received sham and the experimental rats received a single i.p injection of STZ (35 mg/kg) in 0.1 M citrate buffer pH 4.5. After 72 h, fasting blood glucose levels was monitored and animals having blood glucose levels >150 mg/dl were included in the experiment. Diabetic rats were divided into five groups; one group (Group-II) was fed on a regular diet and considered as diabetic control group. Whereas the other four groups (Group-III & Group-IV) of rats received 5 μM and 50 μM/kg body weight) of **15e** compound. **15e** compound was suspended 2% Tween 80 in saline, is administered p.o. consecutively for 8 weeks and diabetic controls receive 2% Tween 80 in saline as vehicle during this period. Whereas Group-V & Group-VI rats were received Fidarestat 50 μM and Sorbinil 50 μM/kg body weight, respectively. Blood glucose levels were recorded once a week for all the animals after an overnight fasting. Cataract progression in experimental rats was monitored on a weekly basis using slit-lamp microscope (VISIL 02 Excel) and scoring of cataract formation was performed as described previously [41]. At the end of 8 weeks, the rats were sacrificed by CO_2 asphyxiation and the lenses were dissected by posterior approach. Animal care and experimental protocols were approved by the University Animal Ethical Committee.

5.5. Statistical analysis

The results were expressed as mean ± SD of 5 replicates and were subjected to one way analysis of variance (ANOVA) followed by Post Hoc Test. To analyze this data we have used the SPSS 15.0 version. Data was analyzed by Prof. V.V. Hara Gopal, Department of Statistics, Osmania University, Hyderabad.

Acknowledgement

We thank Dr. P. R. Krishna (Asst. Prof. of Chemistry, IIT-Roorkee) for helpful discussions. We also extend our thanks to UGC, Osmania University & CFRD-OU facilities for providing infrastructure and HeteroDrugs Pvt. Ltd. Hyderabad for financial assistance to G. Gudipudi.

References

[1] M. Brownlee, Nature 414 (2001) 813–820.
[2] D.M. Nathan, N. Engl. J. Med. 328 (1993) 1676–1685.
[3] P.J. Oates, Curr. drug targets 9 (2008) 14–36.
[4] J.H. Kinoshita, Investig. Ophthalmol. 4 (1965) 786–799.
[5] S.K. Srivastava, K.V. Ramana, A. Bhatnagar, Endocr. Rev. 26 (3) (2005) 380–392.
[6] K.P. Anil, R.G. Bhanuprakash, Eye Res. 85 (2007) 739–740.
[7] S.K. Srivastava, U.C. Yadav, A.B. Reddy, A. Saxena, R. Tammali, M. Shoeb, N.H. Ansari, A. Bhatnagar, M.J. Petrash, S. Srivastava, K.V. Ramana, Chemico-Biol. Interact. 191 (1–3) (2011) 330–338.
[8] R. Van Heyningen, Nature 184 (4681) (1959) 194–195.
[9] H.G. Hers, Biochim. Biophys. Acta 22 (1956) 202–203.
[10] Z. Hashim, S. Zarina, J. Diabetes its Complicat. 26 (2012) 275–279.
[11] J.H. Kinoshita, C. Nishimura, Diabetes/metab. Rev. 4 (4) (1988) 323–337.
[12] J.J. Harding, Cataract: Biochemistry, Epidemology, and Pharmacology, first ed., 1991.
[13] R. Michael, A.J. Bron, Phil. Trans. R. Soc. B 366 (2011) 1278–1292.
[14] R. Kikkawa, I. Hatanaka, H. Yasuda, N. Kobayashi, Y. Shigeta, H. Terashima, T. Morimura, M. Tsuboshima, Diabetologia 24 (4) (1983) 290–292.
[15] K. Sestanj, F. Bellini, S. Fung, N. Abraham, A. Treasurywala, L. Humber, N. Simard-Dequesne, D. Dvornik, J. Med. Chem. 27 (3) (1984) 255–256.
[16] B.L. Mylari, E.R. Larson, T.A. Beyer, W.J. Zembrowski, C.E. Aldinger, M.F. Dee, T.W. Siegel, D.H. Singleton, J. Med. Chem. 34 (1) (1991) 108–122.
[17] S. Ao, Y. Shingu, C. Kikuchi, Y. Takano, K. Nomura, T. Fujiwara, Y. Ohkubo, Y. Notsu, I. Yamaguchi, Metabolism 40 (1) (1991) 77–87.
[18] J.B. Jaspan, K. Herold, C. Bartkus, Am. J. Med. 79 (5) (1985) 24–37.
[19] S.P. Spielberg, N.H. Shear, M. Cannon, N.J. Hutson, K. Gunderson, Ann. Intern. Med. 114 (9) (1991) 720–724.
[20] K. Mizuno, N. Kato, M. Makino, T. Suzuki, M. Shindo, J. Diabet. Complicat. 13 (1999) 141–150.
[21] N. Giannoukakis, Drug Eval. Curr. Opin. Investig. Drugs 7 (10) (2006) 916–923.
[22] S.D. Varma, I. Mikuni, J.H. Kinoshita, Science 188 (4194) (1975) 1215–1216.
[23] (a) O.A. Barski, K.H. Gabbay, C.E. Grimshaw, K.M. Bohren, Biochemistry 34 (1995) 11264–11275;

(b) S.P. Spielberg, N.H. Shear, M. Cannon, N.J. Hutson, K. Gunderson, Ann. Intern. Med. 114 (1991) 720–724.
[24] T. Matsumoto, Y. Ono, A. Kuromiya, K. Toyosawa, Y. Ueda, V. Bril, J. Pharmacol. Sci. 107 (2008) 340–348.
[25] (a) A. Urzhumtsev, F. Tete-Favier, A. Mitschler, J. Barbanton, P. Barth, L. Urzhumtseva, J.F. Biellmann, A. Podjarny, D. Moras, Structure 5 (1997) 601–612;
(b) Peter F. Kador, Jin H. Kinoshita, Norman E. Sharpless, J. Med. Chem. 28 (7) (1985) 841–849.
[26] O. El-Kabbani, C. Darmanin, M. Oka, C. Schulze-Briese, T. Tomizaki, I. Hazemann, A. Mitschler, A. Podjarny, J. Med. Chem. 47 (2004) 4530–4537.
[27] E.I. Howard, R. Sanishvili, R.E. Cachau, A. Mitschler, B. Chevrier, P. Barth, V. Lamour, M. Van Zandt, E. Sibley, C. Bon, D. Moras, T.R. Schneider, A. Joachimiak, A. Podjarny, Proteins 55 (2004) 792.
[28] H. Steuber, M. Zentgraf, C. Gerlach, C.A. Sotriffer, A. Heine, G. Klebe, J. Mol. Biol. 363 (2006) 174–187.
[29] M. Stefek, M. Soltesova Prnova, M. Majekova, C. Rechlin, A. Heine, G. Klebe, J. Med. Chem. 58 (2015) 2649–2657.
[30] G. Gudipudi, S.R. Sagurthi, S. Perugu, G. Achaiah, G.L.D. Krupadanam, Rsc Adv. 4 (2014) 56489–56501.
[31] (a) M. Casagrande, A. Barteselli, N. Basilico, S. Parapini, D. Taramelli, A. Sparatore, Bioorg. Med. Chem. 20 (2012) 5965–5979;
(b) C. Zhou, M. Garcia-Calvo, S. Pinto, M. Lombardo, Z. Feng, K. Bender, K.D. Pryor, U.R. Bhatt, R.M. Chabin, W.M. Geissler, Z. Shen, X. Tong, Z. Zhang, K.K. Wong, R.S. Roy, K.T. Chapman, L. Yang, Y. Xiong, J. Med. Chem. 53 (2010) 7251–7263.
[32] A. Beyer-mears, E. Cruz, Diabetes 34 (1985).
[33] M. Stefek, V. Snirc, P.O. Djoubissie, M. Majekova, V. Demopoulos, L. Rackova, Z. Bezakova, C. Karasu, V. Carbone, O. El-Kabbani, Bioorg. Med. Chem. 16 (2008) 4908–4920.
[34] K.J. Rees-Milton, Z. Jia, N.C. Green, M. Bhatia, O. El-Kabbani, T.G. Flynn, Arch. Biochem. Biophys. 335 (1998) 137–139.
[35] (a) P.F. Kador, J.H. Kinoshita, N.E. Sharpless, J. Med. Chem. 28 (1985) 841–849;
(b) S. Suzen, E. Buyukbingol, Curr. Med. Chem. 10 (2003) 1329–1352 cR. Kikkawa, I. Hatanaka, H. Yasuda, N. Kobayashi, Y. Shigeta, H. Terashima, T. Morimura, M. Tsuboshima, Diabetologia 1983, 24, 290-292.
[36] (a) O. El-Kabbani, P. Ramsland, C. Darmanin, R.P. Chung, A. Podjarny, Proteins 50 (2003) 230–238;
(b) O. El-Kabbani, D.K. Wilson, M. Petrash, F.A. Quiocho, Mol. Vis. 4 (1998) 19.
[37] K.M. Bohren, C.E. Grimshaw, C.J. Lai, D.H. Harrison, D. Ringe, G.A. Petsko, K.H. Gabbay, Biochemistry 33 (1994) 2021–2032.
[38] (a) O. El-Kabbani, C. Darmanin, T.R. Schneider, I. Hazemann, F. Ruiz, M. Oka, A. Joachimiak, C. Schulze-Briese, T. Tomizaki, A. Mitschler, A. Podjarny, Proteins 55 (2004) 805–813;
(b) O. El-Kabbani, V. Carbone, C. Darmanin, M. Oka, A. Mitschler, A. Podjarny, C. Schulze-Briese, R.P. Chung, J. Med. Chem. 48 (2005) 5536–5542.
[39] (a) Kwangseok Ko, Youngdo Won, Bioorg. Med. Chem. 13 (2005) 1445–1452;
(b) Bhawna Vyas, Manjinder Singh, Maninder Kaur, Malkeet Singh Bahia, Amteshwar Singh Jaggi, Om Silakari, Baldev Singh, J. Mol. Graph. Model. 59 (2015) 59–71;
(c) Chanin Nantasenamat, Teerawat Monnor, Apilak Worachartcheewan, Prasit Mandi, Chartchalerm Isarankura-Na-Ayudhya, Virapong Prachayasittikul, E. J. Med. Chem. 76 (2014) 352–359;
(d) Love Kumar Soni, Satish G. Kaskhedikar, Arch. Pharm. Chem. Life Sci. 339 (2006) 327–331.
[40] (a) Peter F.Kador, PengZhang, JunMakita, ZifengZhang, ChangmeiGuo, JamesRandazzo, HiroyoshiKawada, NeenaHaider, KarenBlessing. PLoS One 7(12): e49422. (b) Peter F. Kador, Daniel Betts, Milton Wyman, Karen Blessing, James Randazzo, Am. J. Vet. Res. 67 (10) (2006) 1783–1787.
[41] P. Suryanarayana, P.A. Kumar, M. Saraswat, J.M. Petrash, G.B. Reddy, Mol. Vis. 12 (10) (2004) 148–154.